

UC Berkeley

UC Berkeley Previously Published Works

Title

Parametric study of solid-solid translucent phase change materials in building windows

Permalink

<https://escholarship.org/uc/item/2vw3f5wm>

Authors

Gao, Yuan
Zheng, Qiye
Jonsson, Jacob C
[et al.](#)

Publication Date

2021-11-01

DOI

10.1016/j.apenergy.2021.117467

Peer reviewed

Parametric study of solid-solid translucent phase change materials in building windows

Yuan Gao^{†,1}, Qiye Zheng^{†,1,2}, Jacob C. Jonsson,¹ Sean Lubner,¹ Charlie Curcija,¹ Luis Fernandes,¹ Sumanjeet Kaur*,¹ Christian Kohler*¹

¹ Lawrence Berkeley National Laboratory, Berkeley, California

² Mechanical Engineering, University of California at Berkeley

*Email: skaur1@lbl.gov, cjkohler@lbl.gov

[†]These authors contributed equally: Yuan Gao, Qiye Zheng

Abstract

Thermal energy storage and solar radiation management are crucial to improve the sustainability and energy efficiency of buildings. Compared with the implementation of phase change materials (PCMs) in opaque components, the energy saving potential of incorporating PCMs in transparent glazing windows is much less studied and not well understood. Here we present a comprehensive parametric study of novel PCM windows for building energy saving with a focus on optimizing and quantitatively distinguishing the contributions from the optical and thermal properties of the PCM, which is particularly useful for the design of solid-solid PCM windows. We investigate a reference commercial office building using EnergyPlus by developing an equivalent model of our PCM window that is compatible with EnergyPlus's modeling capabilities. Compared with a clear-clear double-pane window, the integration of 3 mm solid-solid PCMs with optimal properties in warm, mixed, and cold climates can respectively save up to 17.2%, 14.0%, and 5.8% energy for the HVAC (heating, ventilation, and air conditioning) system, and 9.4%, 6.7%, and 3.2% energy for the whole building. We also demonstrate that these energy savings are most sensitive to the solar absorptance of PCMs for all three climates. The optimal transition temperature varies with climate and is related to the climate and solar radiation heat gain. Other issues are also briefly discussed, such as hysteresis, window orientations, and the effect of interior lighting. Although the optimal PCM windows show energy saving performance comparable with low-emissivity windows, the PCM windows provide a unique advantage in terms of shifting HVAC loads which can provide benefits to the electrical grid.

Nomenclature

Notations		Abbreviations/subscripts	
l	Thickness (m)	CondFD	Conduction finite difference
S	Area (m ²)	WWR	Window-to-wall ratio
τ	Solar transmittance	DOE	Department of Energy
α	Solar absorptance	HVAC	Heating, ventilation, and air conditioning
r	Solar reflectance	PCM	Phase change material
ρ	Density (kg/m ³)	tPCM	Translucent phase change material
k	Thermal conductivity (W/(m K))	ePCM	Equivalent opaque phase change material
c_p	Specific heat capacity (J/(kg K))	TIM	Transparent insulation material
C_{th}	Thermal mass (J/K)	WG	Window glazing
m	Mass (kg)	eWG	Equivalent window glazing
R_S	Ratio of the area of equivalent PCM to that of window glazing	WG+tPCM	Window glazing integrated with translucent phase change material
E	Energy consumption per conditioned building area (MJ/m ²)	TIM+ePCM	Transparent insulation material integrated with equivalent opaque phase change material
ΔE	Energy saving per conditioned building area (MJ/m ²)	TES	Thermal energy storage
ΔH	Latent heat (kJ/kg)	CO ₂	Carbon dioxide
T_c	Central phase change temperature (°C)	GU	Glazing unit
ΔT_{pc}	Temperature breadth of phase change (°C)	DGU	Double-glazing unit
ε	Contribution share of energy saving (%)	TGU	Triple-glazing unit
T_m	Melting temperature	DPW	Double-pane window
T_f	Freezing temperature	TPW	Triple-pane window

1. Introduction

Buildings account for about 28% and ~36% of total end-use energy consumption in the U.S. and the world respectively and generate ~40% of the energy and process-related global CO₂ emission [1], [2]. At present, 50-60% of the total energy in commercial buildings is used by heating, ventilating, and air conditioning (HVAC) systems [1], which account for the largest energy expense among all sectors [3], [4], and are expected to further increase over the coming decade [5], [6]. It is thus crucial to develop efficient and sustainable technologies for building thermal energy management.

To this goal, increasing the insulation and thermal mass of building envelopes are believed to be two promising design solutions [7], [8]. Thermal energy storage (TES) utilizing phase change materials (PCMs), which increases the building thermal mass with their large latent heat, has been one of the promising technologies in buildings to manage the indoor temperature and enhance the HVAC efficiency (by addressing the discrepancy between energy supply and demand) for over seven decades [3], [9]. With many other benefits, e.g. lightweight and considerable sensible heat [8], [10], implementation of PCMs in opaque building envelopes is widely studied and was reported to provide the benefits of reducing HVAC energy consumption, shifting the cooling/heating load to off-peak hours and optimizing the interior temperatures control in experiments [11], [12].

Prior research of PCM in buildings mainly investigated the incorporation of solid-liquid (S-L) PCM by immersion, encapsulation or shape stabilized composite addition into opaque building elements such as concrete, brick, and board in walls, floors, and roofs. For example, Lee et al. studied the effect of integrating a thin PCM layer into the residential building walls in house-scale experiment which they found to provide 30–50% reductions and 2–6 h delay in peak heat flux, and a maximum daily heat load reductions of 3–27% compared with the case without the PCM [13]. Karim et al. developed a hollow concrete floor panel with PCM enclosed in its cavities to increase the floor thermal inertia, which increased its ability to store thermal energy, shifted the peak loads by ~1 h, and improved the stability of indoor temperature [14]. The results showed that the macro encapsulated PCM panel can reduce the interior temperature at the room center and at the internal surface of the panel by 4.7°C and 7.5°C. More recently, Abden et al. experimentally studied the thermal performance of a composite PCM-incorporated gypsum board false ceiling for summer cooling load reduction, which was demonstrated to reduce the room temperature by 4.9°C in the first day of the experiment and an average reduction of 3.5°C was obtained during the three-day experiment compared with an identical chamber of standard gypsum board [15]. Li et al fabricated a composite PCM wallboard containing three types of PCMs with different melting points to maintain thermal comfort and increase energy saving under different climate conditions. The results showed high energy saving by up to 30% for the wallboard-based PCM with reasonable thermal control of temperature fluctuations compared with the standard gypsum wallboard [16].

These favorable results are also validated in full scale building simulations. For example, Soares et al. investigated the impact of installing PCM drywalls on the energy performance of single-zone

residential buildings and found that 10% to 62% energy consumption reductions can be achieved by inclusion of PCM depending on the climate zone [17]. Hu and Yu simulated the performance of a PCM embedded wall board in five different climate conditions using EnergyPlus in terms of total energy saving and CO₂ emission reduction, with varied PCM board type and thickness [18]. They found that the incorporation of PCM could save energy consumption by 6% and reduce CO₂ emissions by 1% in the warm climate buildings. More comprehensive review on the PCM in opaque building elements can be found elsewhere [3], [19], [20].

In contrast to opaque components [10], [21], the incorporation of PCM in transparent building elements is a less studied field [22] that could also play an important role in energy saving [23]. In fact, glazing units are responsible for about 10% of the total energy consumption within buildings through heat loss or solar gain due to their poor thermal performance and optical transparency [24]. Compared with chromic materials which are mainly used to tune the incoming solar radiation [25], (semi)transparent PCMs (e.g. paraffin wax, salt hydrates) can provide extra benefits such as load shifting and peak reduction via TES in building envelopes. Many prior experiments showed that the inclusion of PCM in a double glazing or triple glazing unit (DGU or TGU, sometimes referred as double or triple pane window, DPW, TPW) can effectively reduce the interior temperature fluctuation and undesirable heat exchange through the window [26], [27].

However, two issues remain unsolved in the development of such TES with PCM in glazing units. First, the actual energy savings at the whole building level are still not clear. Previous small-scale simulations (e.g. simplified 1D model for a glazing unit or a room) [28], [29] or test chamber experiments [30], [31] could only approximately mimic the PCM modulation of inner temperature and heat flux without quantitative investigation of energy savings [32], [33]. For example, early research by Goia et al. combined small control chamber experiment and numerical simulation to study the performance of DGU with S-L PCMs [34]–[36]. They demonstrated the effect of PCMs to reduce the solar transmission, moderate the heat flux and indoor temperature. Bianco et al. reported a numerical and experimental assessment of a novel dynamic PCMs based solar shading with different colors which can reduce the daily cooling energy by about 40% and provide a 3 h time shift of the heat fluxes peak crossing the system [37]. Hu et al. proposed and studied a PCM enhanced ventilated window system where PCM is placed in an opaque plate beneath the transparent glazing unit for ventilation preheating/precooling purposes for building energy saving [38]. By numerical modeling and a full-scale experiment, they found that the inclusion of PCM in ventilation systems can decrease the demand for summer cooling energy by 27% to 38% and winter heating energy by 10% to 29%. Li et al. investigated photothermal properties of a paraffin-containing DGU using a solar simulator experiment in a laboratory with a focus on the non-gray optical characteristics of the paraffin and the glass and found that the transmitted solar energy decreased from 67.6% to 45.9% when the PCM thickness increased from 6 to 25 mm [39]. Ahmed et al. studied a sliding smart window integrated with vacuum insulation, photovoltaic, and PCM using ANSYS finite element modelling and found that adding PCM shifted the peak energy transferred to the indoor by 2-5 h [40]. Notably, none of the aforementioned work studied the thermal energy performance of a glazing unit with semi-transparent PCM directly incorporated in

a whole building scale in conjunction with the simulation of other energy components such as the HVAC and the lighting system. The only preliminary building scale simulations by Bionda et al. using IDA ICE showed that the integration of translucent PCM modules in the considered building scenarios can lead to energy savings in the order of about 0-9% (cooling) and 7-10% (heating) [41]. However, they only considered one type of S-L PCM (Calcium chloride hexahydrate) and one climate zone (Zürich, Switzerland). Also, all prior work on window glazing with PCM focused on the S-L phase transition as far as we know.

Second, the mechanism of the energy savings of using PCM regarding its optical and thermal contributions to the energy performance of the glazing system is not well understood. Experimental research on this topic focused on S-L PCMs which undergo a large change in visible optical transmission from a hazy and semi-translucent state in solid phase to transparent state in liquid phase [33], [42]. Practically, this issue affects the indoor view and may act as a dealbreaker for the application of PCM windows in residential and commercial buildings [22], [23]. More importantly, none of the prior experiments distinguished the energy saving by solar absorption from that by thermal mass and latent heat, probably owing to the difficulty in preparing control groups (e.g., a tinted window with solar optical properties that match the PCM). Hence a natural question is: how does a PCM window perform compared with a tinted window with the same thermal insulation? The sole prior building level simulation on the energy savings of S-L PCM windows considered one case of PCM with optical properties that differs in the two states without comprehensive parametric control simulations and cannot resolve the question here [41].

On the other hand, PCM with solid to solid (S-S) phase transition tend to have more consistent optical properties, no leakage problem and many other advantages over S-L PCMs and has received increasing research attention on the TES application in building envelopes (see section 2.1) [43]. To date, there is no direct experimental research that incorporates S-S PCM in building to evaluate their compatibility and performance in TES applications. In addition, a comprehensive numerical research on the potential performance of S-S PCMs for building energy applications especially for window glazing is still lacking [44], [45]. Thus, our research here serves to evaluate the potential of S-S PCM in window glazing for building energy saving and further guide the design of materials.

Here, we systematically investigate the energy savings of PCM windows with varied thermal and optical PCM properties with a parametric sweep using the EnergyPlus whole building simulation software. We overcome EnergyPlus's inability to simulate translucent PCMs by developing a thermally equivalent model and validate it. We also use parametric study with multiple control groups to tackle the two issues mentioned above. Six material parameters are investigated and optimized: solar absorptance (α_{iPCM}), thermal conductivity (k), latent heat (ΔH), heat capacity (c_p), phase change temperature (T_c), and the temperature breadth of the phase change (ΔT_{pc} , note this is not the thermal hysteresis) of PCMs. We show that the inclusion of PCM in clear-clear double-pane windows can effectively save from 5.8% to 17.2% energy consumption of HVAC systems for commercial buildings in different climate zones with proper material properties that are

achievable in organic semi-transparent PCMs. Furthermore, the energy saving is strongly influenced by the optical properties of the PCM layer. For optimal PCMs, 60.5-70.4% of the energy saving results from the reduction of solar heat gain due to the absorption of PCM. Nevertheless, latent heat still contributes a considerable portion of 14.8-22.9%. Other issues, such as hysteresis and thermochromic effects, window orientations, and balance with interior lighting consumption, are also briefly discussed. We show that the PCM thermal hysteresis can modulate the heat releasing process and further save cooling energy. The dependence of the optimal PCM properties on the building room orientation is also studied. Our simulation is useful for the development of next-generation solid-solid (S-S) PCMs which have the potential of a consistent optical semi-transparency in the two states and various other advantages over S-L PCMs. The novelty of this work is that 1) it provides a new validated equivalent model to simulate the energy savings from translucent PCM windows using Energy Plus. This feature of simulating PCM windows is currently missing in Energy Plus. 2) By using our model, we optimize and demonstrate the effect of transition temperature, different optical and thermal properties of PCM window on energy savings and peak shifting for different climates and reveal the mechanisms behind accordingly. 3) In addition, we provide a comprehensive numerical research on the potential performance of S-S PCMs for building energy applications especially for window glazing, which is still lacking [44], [45]. Thus, our research here serves to evaluate the potential of S-S PCM in window glazing for building energy saving and further guide the design of PCM windows to achieve an optimized energy saving effect under practical building implementation constraints.

2. Method

2.1 Material perspective

To optimize PCMs for window applications, it is fundamental to take into account the material properties to identify a realistic scope of parametric study. For TES applications of PCMs, the latent heat (ΔH) determines the energy storage density while other thermal properties, i.e., thermal conductivity (k) and heat capacity (c_p) determine the charging/discharging rate and hence the power density [46], [47]. The intrinsic thermal conductivity (k) of PCMs, especially organic PCMs, is low (0.1-1 W/(m K)) [46], which can be enhanced by the incorporation of high- k components into the PCM to exceed 1 W/(m K) easily [48]. The latent heat of organic PCMs relevant to our study typically ranges between 90 to 250 kJ/kg [3]. On the other hand, unlike PCMs for opaque building components and some TES applications [49], which charge through heat conduction, optical properties, especially solar absorptance (α_{tPCM}), are important for PCMs in glazing units (GUs). There have been multiple reports on the tuning of the optical absorption of organic PCMs by synthetic control of the chemistry [50], [51] or the integration of optical absorbers [52], [53]. The resulting transmission of the PCMs can be varied significantly (e.g., for paraffin wax the transmission decreases from 0.9 to <0.05 in the liquid state with the addition of CuO nanoparticles [54]).

As discussed in the introduction, common commercial PCMs such as paraffin wax or salt hydrates [22] are S-L PCMs, which suffer from a significant change of the specific volume and the variation of optical properties through their phase transition that would impair visibility through windows. In addition, the potential for liquid leakage of these PCMs (e.g. PCM in window shutters [55]) is another challenge for their application to windows, requiring the use of microencapsulation and composite structure with porous material framework which also inevitably reduce the effective latent heat, ΔH , and change the optical properties of the PCMs [56]. In comparison, S-S PCMs possess advantages such as no leakage, less phase-segregation, and small volume change. These features enabled their encapsulation-free implementation and an extended durability upon thermal cycling, which are important for building applications that require long-term performance.

Nowadays, S-S PCMs is attracting increasingly wide attention for TES applications (e.g., passive solar architectural applications, waste heat recovery, and concentrated solar power) [57], [58] and great progress has been made to optimize their transition temperature and ΔH [59], [60]. For building applications, Guldentops et al. numerically investigated an adaptive passive solar building enclosure system using a thin layer of polymeric S-S PCM as a coating onto a highly reflective exterior façade layer [61]. The S-S PCM remains in opaque crystalline phase which absorbs solar radiation and conduct heat to the room to reduce heating loads during winter and transitions to amorphous and transparent state at elevated outdoor temperatures during summer which exposes the reflective layer to reflect solar radiation and reduce cooling loads. Yan et al. experimentally studied the transition temperature and latent heat of a series of binary organic S-S PCM which can be suitable for the implementation in building walls [62]. For window applications, on the other hand, S-S PCMs have the potential to be engineered to maintain a relatively consistent optical property through the transition with future research which is challenging for S-L PCMs [43].

Recently, our team developed a modified poly(ethylene glycol) (PEG) based S-S PCM with ΔH around 100 kJ/kg and a transition temperature between 25-40°C; and its optical properties can be potentially be tuned in the polymerization process [63]. Therefore, it is reasonable to expect that the PCM properties in our parametric study (Table 2) can be realized in S-S polymer with nearly constant optical properties in the low and high temperature state with further material development.

2.2 Reference office building

To evaluate the thermal performance of transparent PCMs in a typical building environment, we built a model of a commercial office space, adapted from the U.S. Department of Energy (DOE) reference model for a medium-size office building [4]. As shown in Figure 1a, for the purposes of the modeling of energy transfer in the space, the reference office used in this study is divided into three zones, among which only one contains an exterior south-facing wall with fenestration, where the PCM-window or its counterparts (clear-clear or low-e-clear double-pane window) in this study are installed. The other two zones in the model are the interior part of the space and the ceiling plenum. The window-to-wall area ratio (WWR) of the façade is fixed at 0.5. The net conditioned building area is 178.4 m². Important geometric parameters of the building are labeled in Figure 1a.

In this study, the energy consumption (E) or savings (ΔE) refers to energy per conditioned building (floor) area in the unit of MJ/m² unless otherwise stated. Several end-use categories contribute to the total site^a energy use, including heating, cooling, interior lighting, interior equipment, and fans. Electricity and natural gas (for heating) are the only two energy sources used in this reference office. No feedback control algorithm for lighting or equipment is applied to this study. In other words, as we implement different windows with or without PCMs in the reference office, the energy consumption by interior lighting and equipment remains constant at 121.7 MJ/m² and 128.9 MJ/m², respectively. At the same time, varying the type of windows impacts the end-use categories of heating, cooling, and fans. Here we use the term of HVAC (heating, ventilation, and air conditioning) to indicate these three categories as a whole. Since the other two end-use categories (interior lighting and equipment) have fixed consumption, the ΔE of the HVAC caused by varying window configurations is the same as total ΔE for the building model.

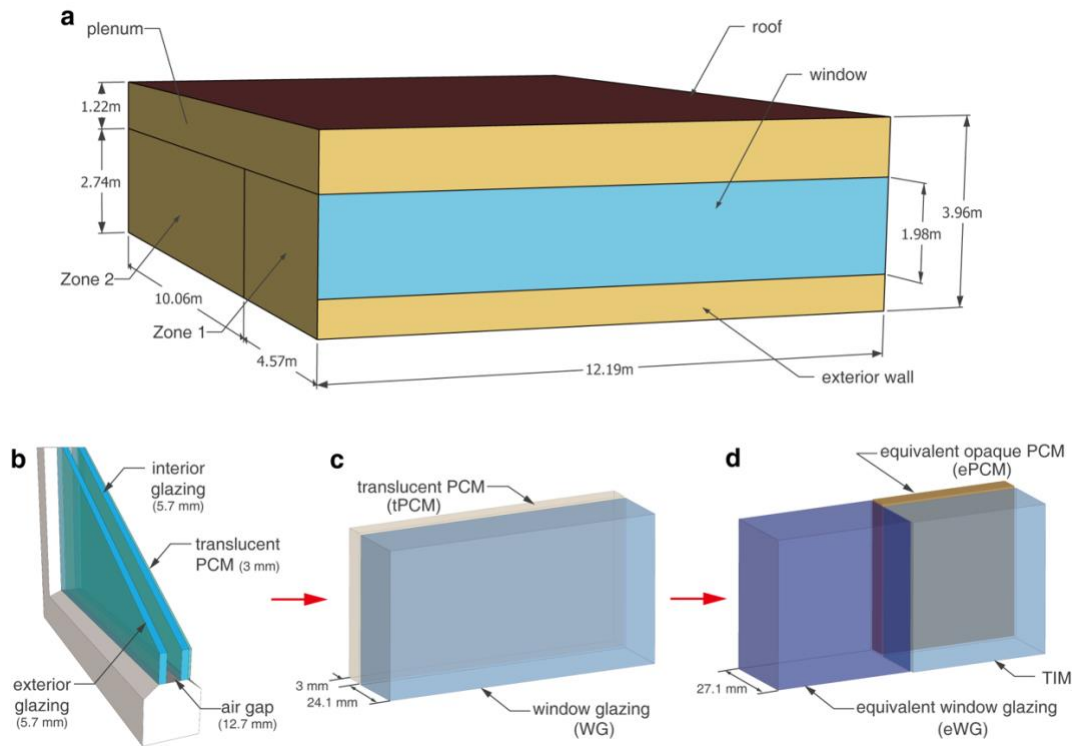


Figure 1 Reference commercial office building and the equivalence of the PCM window in EnergyPlus. **a.** Schematic diagram of office room with a south-facing window. **b.** Real system: clear-clear double-pane window with a PCM layer between the air gap and the interior glazing. **c.** Thermal model: translucent PCM (tPCM) integrated with window glazing (WG). Note that the thickness of the tPCM layer is exaggerated for visual clarity. **d.** Thermally equivalent model in EnergyPlus (which cannot simulate

^a Site energy is used here to distinguish energy used at the building site from the amount of energy needed at the source of energy production to provide the energy to the site. i.e., site energy does not account for production, transmission or other distribution losses.

transparent PCMs), including equivalent window glazing (eWG), transparent insulation material (TIM, which has the same optical and thermal properties as the WG in c), and equivalent opaque PCM (ePCM).

Three cities are selected for the EnergyPlus simulation to represent three different types of climates in the world, i.e., warm (Houston, Texas, 30° 0' 0" N, 95° 22' 12" W, 29 m altitude), mixed (Washington, D.C., 38° 58' 48" N, 77° 28' 12" W, 82 m altitude), and cold (Minneapolis, Minnesota, 44° 52' 48" N, 93° 13' 48" W, 254 m altitude) climates (see Supplementary Note 1). Detailed monthly statistics of solar radiation and air temperature can be found in Supplementary Table 2.

Hourly operation schedules for a medium-size office building are applied to the heating and cooling temperature setpoint (Figure 2a) [4]. A simplified hourly operation schedule, which is set at 24°C for all hours, was used for the cooling temperature setpoint for the purpose of making it more straightforward to understand the energy impact of PCM behavior as distinct from other schedule-related variations in HVAC energy use. The hourly lighting schedules (Figure 2b) in this model are the same as included in the DOE reference buildings [4].

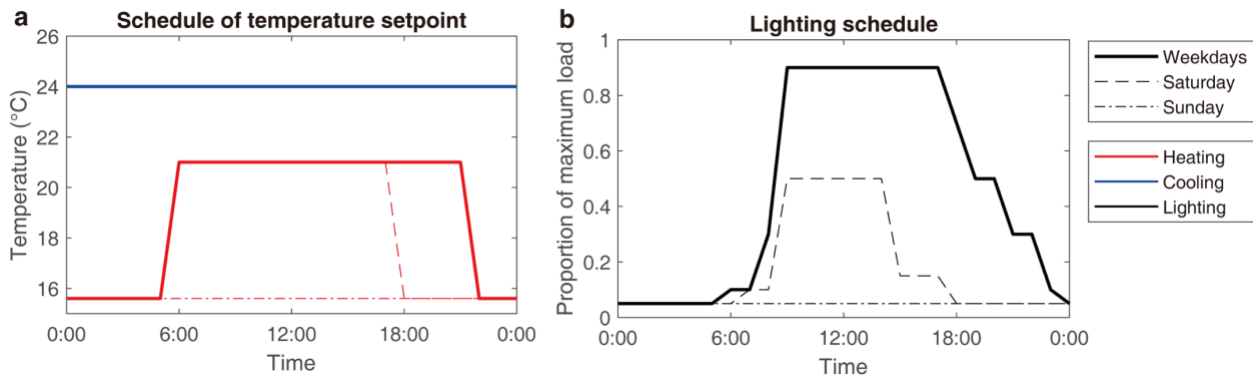


Figure 2 a. Temperature schedule and b. lighting schedule

Note that in this model the interior lighting energy is defined by lighting input power per zone floor area and a standard lighting schedule for commercial office buildings. It indicates two assumptions: (1) lighting control is purely based on a time schedule instead of daylighting conditions; and (2) the illuminance level is always adequate for users in spite of daylighting. Therefore, it is reasonable to presume that interior lighting energy will not be affected by introducing PCM windows because the designed lighting power and schedules can satisfy the illumination demand during the daytime hours, even when the daylighting goes down to zero. Additionally, to understand the impact of PCM integration on lighting, we consider the situation in which interior lights are dimmable according to a daylighting reference point. Simulation results show that the increased interior lighting energy by PCM windows is negligible compared with the HVAC saving. Detailed explanation can be found in Supplementary Note 2.

2.3 Equivalent model of PCM window in EnergyPlus

The simulation of PCM in opaque building components using the open-source tool EnergyPlus (based on enthalpy method) has been validated by both modeling and experiment a few years ago [64], [65] and now includes the modeling of hysteresis of PCMs. At present the commercial software of IDA-ICE, which is not fully and publicly available, is the only tool capable of addressing both opaque and transparent building envelope components that integrate PCMs. However, the potentials and limitations of the IDA-ICE simulation have not been extensively communicated and a comprehensive validation is lacking [66]. To facilitate the applicability and future validation of our simulation, we chose to use EnergyPlus here.

The schematic diagram of the PCM window in this study is shown in Figure 1b. In an actual window, the translucent PCM layer would be placed on the inside surface of the interior glazing of a clear-clear double-pane window (DPW). To simplify the simulation model, the optical properties of the clear-clear DPW are calculated using WINDOW, a software package for calculating the thermal and solar optical of windows [67], and fed to EnergyPlus as an equivalent single-glazing window, as shown in Figure 1c. For the purposes of building energy modeling, the simplified model of translucent PCM integrated with window glazing (WG) in Figure 1c has equivalent optical and thermal behaviors to the PCM window in Figure 1b. The optical and thermal properties of the DPW (three-layer glass - air - glass as a whole) in Figure 1b are equivalent to the properties of WG in Figure 1c (see Supplementary Table 4).

EnergyPlus simulates the thermal effect of the PCMs with a conduction finite difference (CondFD) solution algorithm which has been previously validated [64], [65], [68]. However, there are two challenges in simulating PCMs windows with EnergyPlus. Firstly, as mentioned above, the current EnergyPlus PCM module algorithm is designed for the use of PCMs in opaque building components, i.e., the transmittance of PCM is fixed at zero in EnergyPlus. Therefore, (semi)transparent PCMs cannot be directly simulated in the current version of EnergyPlus (9.4.0). Secondly, EnergyPlus does not account for thermal mass in glazing.

To overcome these challenges and make it possible to simulate a (semi)transparent PCM window in EnergyPlus, we propose a model that divides the simplified window (Figure 1c) into two components which, together, behave in an equivalent way to the PCM window under study. We introduce here the concept of a “transparent insulation material” (TIM)^b, which can be defined as an exterior movable insulation object in EnergyPlus. The behavior of the exterior TIM layer is also simulated in EnergyPlus using the CondFD solution algorithm, therefore properly accounting for thermal mass effects in the glazing (non-PCM) part of the window. The key in this equivalent model is determining the correct ratio between the areas of its two parts so that it has net optical properties that are equivalent to the realistic transparent PCM case (thermal properties are adjusted accordingly).

^b TIM is defined by the object name “SurfaceControl:MovableInsulation” in EnergyPlus. The properties of TIM are specified by the “WindowMaterial:Glazing” object.

The equivalent model is shown in Figure 1d, where the window is split into two parts. The transparent part, which is occupied by equivalent window glazing, accounts for the transmission of solar radiation through the simplified window shown in Figure 1c and a fraction of absorption of solar radiation in WG, i.e., the glazing (non-PCM) part of the simplified window. The opaque part, which is composed of TIM and opaque PCM, accounts for the amount of solar radiation that would be absorbed by the translucent PCM and the remaining fraction of glazing absorption in WG. The properties of the objects in the equivalent model (Figure 1d) are calculated in such manner that the model is equivalent to the simplified model (Figure 1c) in terms of window dimensions, absorbed and transmitted solar energy, thermal resistance and thermal mass. In Table 1, we summarize the derived equations that calculate the parameters of equivalent layers in Figure 1d. Detailed calculations of object properties in the equivalent model are introduced in Appendix A-D.

Table 1 Summary of parameters of equivalent layers in Figure 1d

Categories	Parameters	eWG	ePCM	TIM
Dimensions	Thickness (l)	$l_{WG} + l_{tPCM}$	l_{tPCM}	l_{WG}
	Area (S)	$S_{WG}(1 - R_S)$	$S_{WG}R_S$	$S_{WG}R_S$
Optical	Absorptance (α)	α'_{WG}	1	α'_{WG}
	Reflectance (r)	$r'_{WG+tPCM}$	0	$r'_{WG+tPCM}$
	Transmittance (τ)		$1 - \alpha - r$	
Thermal	Thermal conductivity (k)	Appendix Eq. (22)	k_{tPCM}	k_{WG}
	Density (ρ)	-	$\frac{\rho_{tPCM}}{R_S}$	-

To validate our proposed equivalent model of PCM windows in EnergyPlus, we first use our method to reproduce experimental results from literature [31] and found a good agreement between simulation and experimental results. Secondly, we use a step-by-step approach to validate the opaque PCM model, the equivalence of window glazing, and the equivalence of TIM and opaque PCM. We prove that each component of the equivalent model has an acceptable error. In light of these two validations, we can trust the proposed equivalent model of translucent PCM windows in EnergyPlus and use it to evaluate and optimize the PCM windows in buildings. Detailed validation can be found in Supplementary Note 3.

2.4 Simulation variables and cases

The tunable properties of transparent S-S PCMs enable PCM-window applications in a wide range of climates. Practically, it is a challenge to identify the optimal material properties and configuration of the PCM windows for energy savings in buildings without a systematic study to map the effect of all parameters. Thus, we used the aforementioned equivalent models, using batch

processing of computer simulations, to conduct the performance evaluation of PCM windows in buildings. In this study, we select six PCM properties that may have large impacts on the building energy: solar absorptance (α_{tPCM}), latent heat (ΔH), specific heat capacity (c_p), thermal conductivity (k), central phase change temperature (T_c), and temperature breadth of phase change (ΔT_{pc}). We consider a commonly used simplified piecewise linear enthalpy-temperature curve as shown in Figure 3 where four of the variables are defined.^c Note that when we change ΔT_{pc} alone, ΔH is not changed.

The six PCM variables are listed in Table 2, along with the values of each variable. Note that the range of the variables here are reasonable for common PEG or paraffin wax PCMs and should be achievable for S-S PCM as discussed in Section 2.1. The optical α_{tPCM} can be higher than 0.5 but that would decrease the visible light transmittance of the window below a level that is not desirable for most buildings. We also fixed the PCM thickness to 3 mm which is reasonable for the configuration of DPW as shown in Figure 1b. To avoid excessive computational load, the numbers of variable values are limited to ≤ 4 in the preliminary simulation, resulting in 972 combinations. Then further simulations with finer steps are considered to obtain the optimal PCM properties based on the rough results in the preliminary simulation.

Previous research reported that the hysteresis effects of PCM have impacts on the thermal performance of buildings [69]. Though EnergyPlus has an object that describes the material property of phase change hysteresis, the partial melting-freezing cycle of PCM is barely considered in the current version of EnergyPlus (9.4.0). Therefore, the hysteresis effects of PCM are excluded in our analysis, but will be discussed using a daily example, in which a complete melting-freezing cycle of hysteresis PCM happens.

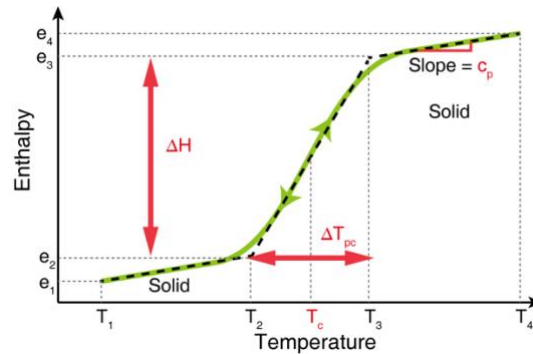


Figure 3 Simplified piecewise linear enthalpy-temperature model of PCM (black dashed line) used in the main part of our simulation to approximate the real enthalpy curve (green line, no hysteresis). Four variables (ΔH , c_p , ΔT_{pc} , and T_c) are labeled.

^c In EnergyPlus, such a simplified curve is defined by four pairs of coordinates (T_i , e_i), where $i = 1, 2, 3, 4$.

Table 2 Six PCM variables and values in the preliminary simulation

PCM variables	Values
α_{tPCM}	0.1, 0.3, 0.5
ΔH (kJ/kg)	50, 150, 250
c_p (J/(kg K))	1200, 1600, 2000
k (W/(m K))	0.1, 0.5, 0.9
T_c (°C)	20, 30, 40, 50
ΔT_{pc} (°C)	2, 10, 18

Note that the PCM variable α_{tPCM} in Table 2 indicates the solar absorption of the single layer translucent PCM while our equivalent model then dictates the value of the solar absorptance of translucent PCM in the WG+tPCM system, α'_{tPCM} , as shown in Figure 1c. Here, we performed optical simulations using the WINDOW software to calculate α'_{tPCM} . The optical parameters values of relevant layers in Figure 1c are listed in Table 3. α'_{tPCM} and $\tau'_{WG+tPCM}$ vary with α_{tPCM} . $r'_{WG+tPCM}$ and α'_{WG} are fixed at 0.12 and 0.04, respectively. The optical properties in the equivalent model are then changed by changing the S_{ePCM} based on Appendix Eq. (19). We elect to use the intrinsic PCM absorption α_{tPCM} in the later discussion in Figure 7 and 8 for better guidance since these values are directly measurable in material development.

Table 3 Optical properties of PCM, window glazing, and WG+tPCM system. The intrinsic absorptance α_{tPCM} and the effective absorptance of the PCM in the system is highlighted.

Optical layer(s)	Parameters	Values			
Single layer tPCM	α_{tPCM}	0.10	0.30	0.50	
	r_{tPCM}	0.06	0.06	0.06	
	τ_{tPCM}	0.84	0.64	0.44	
WG	α_{WG}	0.06	0.06	0.06	
	r_{WG}	0.14	0.14	0.14	
	τ_{WG}	0.80	0.80	0.80	
WG+tPCM system	$r'_{WG+tPCM}$	0.12	0.12	0.12	
	$\alpha'_{WG+tpcm}$	α'_{WG}	0.04	0.04	0.04
		α'_{tPCM}	0.06	0.24	0.42
	$\tau'_{WG+tPCM}$	0.78	0.6	0.42	

Besides studying the total site energy savings (ΔE_{total}) from PCM windows, we propose a method to further break down the contribution to ΔE_{total} by solar absorption (ϵ_α), thermal mass ($\epsilon_{C_{th}}$), and latent heat ($\epsilon_{\Delta H}$) through comparing four cases of window models, shown in Figure 4, while keeping all other aspects of the building model constant.

Case 1 is the base case with clear-clear DPW glazing and no PCM. Case 4 is the same model as shown in Figure 1c with WG+tPCM of core interest in this study, and in which the PCM has both thermal mass and latent heat. Case 2 is a tinted glazing window that has the equivalent solar

absorptance as the WG+tPCM system in Case 4 but no thermal mass. Case 3 is a window with the same thermal mass as in Case 4 but without phase change properties ($\Delta H = 0$ in Figure 3). Cases 2, 3, and 4 have equal solar transmittance (τ) and reflectance (r).

The energy saving, i.e., the difference between Case 1 and Case 4, ΔE_{total} , is then broken down in three parts as shown in the bracket in Eq. (1). By comparing Case 1 and 2, we can estimate how much energy is saved purely by solar absorption and exclude the contribution by thermal mass. Similarly, Case 3 has the same optical properties as Case 2, but has additional thermal mass, however, without latent heat. By comparing Case 2 and Case 3, we can estimate the energy saving by thermal mass and exclude the contribution from the latent heat of the PCM. Lastly, the energy savings from the latent heat can be estimated by comparing Case 3 and 4. Detailed definitions are given by the following equations.

$$\Delta E_{total} = E_{total,1} - E_{total,4} = (E_{total,1} - E_{total,2}) + (E_{total,2} - E_{total,3}) + (E_{total,3} - E_{total,4}) \quad (1)$$

With these energy differences, we can estimate the energy saving contribution from the three factors respectively, as defined below.

$$\varepsilon_{\alpha} = \frac{E_{total,1} - E_{total,2}}{\Delta E_{total}} \times 100\% \quad (2)$$

$$\varepsilon_{C_{th}} = \frac{E_{total,2} - E_{total,3}}{\Delta E_{total}} \times 100\% \quad (3)$$

$$\varepsilon_{\Delta H} = \frac{E_{total,3} - E_{total,4}}{\Delta E_{total}} \times 100\% \quad (4)$$

Note that the total site energy savings (ΔE_{total}) is the same as HVAC energy savings (ΔE_{HVAC}) because other energy uses (interior lighting and equipment) are fixed. Three categories contribute to the HVAC energy savings: heating ($\Delta E_{heating}$), cooling ($\Delta E_{cooling}$), and fans (ΔE_{fans}).

$$\Delta E_{total} = \Delta E_{HVAC} = \Delta E_{heating} + \Delta E_{cooling} + \Delta E_{fans} \quad (5)$$

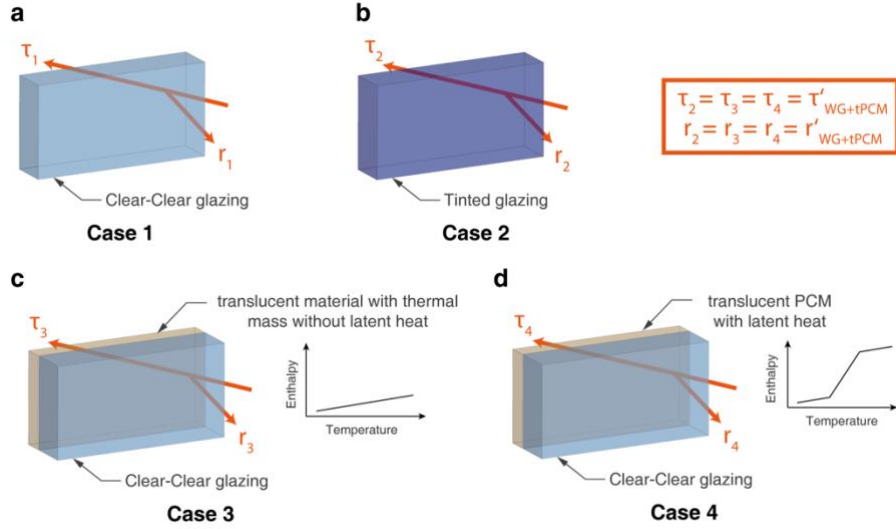


Figure 4 Four window cases that distinguish the energy saving contribution by solar absorption, thermal mass, and latent heat without hysteresis. **a.** Clear-clear DPW with a solar transmittance τ_1 and reflectance r_1 . **b.** Tinted window with a solar transmittance τ_2 and reflectance r_2 . **c.** Clear-clear DPW integrated with a translucent-material layer (τ_3 and r_3) with thermal mass but has no latent heat. **d.** Clear-clear DPW integrated with a translucent-PCM layer (τ_4 and r_4), which has finite latent heat.

3. Results

The optimal properties of PCM windows are obtained by running a preliminary simulation batch (972 combinations of six variables) and a secondary simulation batch (27 extra PCM conditions by varying T_c from 20°C to 50°C with 1°C step) for each climate type. In this section, we first overview the energy savings from the optimal PCM windows that are selected out of the 999 (972+27) PCMs and analyze the sensitivity of energy savings to each PCM variable under different climates. Then, statistics of the primary and secondary simulation batches are presented and analyzed to understand the PCM performance in buildings under different climates. Lastly, we illustrate the cooling and fans loads over the time span of a year, a month, and a day in the warm climate, aiming to show how PCM windows contribute to cutting down the daily peak cooling loads of buildings.

3.1 Overview and energy saving contribution breakdown

The difference in annual energy consumption between a clear-clear DPW (Case 1) and the optimal PCM windows (Case 4) is shown in Figure 5 with regards to total site energy, HVAC, cooling, heating, and fans. The optimal properties of PCM windows used here is optimized by maximizing ΔE_{total} and will be introduced later in Table 5. Among all the three climates, the optimal PCM windows, which, as will be shown later, have a high intrinsic absorption coefficient of 0.5, consume less HVAC energy than the clear-clear DPW. As will be seen, the optimal PCM windows

benefit the annual energy saving mainly by reducing the energy use in cooling and fans; these PCM windows have, however, a negative contribution to heating energy. Note again, based on our assumption, $\Delta E_{total} = \Delta E_{HVAC}$. The annual energy saving rate ($\frac{\Delta E_{total}}{E_{total,1}} \times 100\%$) of total site energy is 9.4%, 6.7%, and 3.2% in the warm, mixed, and cold climates, respectively. Regarding HVAC, the annual energy saving rate ($\frac{\Delta E_{HVAC}}{E_{HVAC,1}} \times 100\%$) is up to 17.2%, 14.0%, and 5.8% in the warm, mixed, and cold climates, respectively. Under the warm (cooling-dominated) climate, the optimal PCM window saves more energy than under other climates.

As shown in the top row in Figure 5, the contributions of PCM windows to the annual energy saving are threefold. The solar absorption plays a major role, accounting for 60.5-70.4% of the annual energy saving. The thermal mass contributes to 9.6-20.8% of the annual energy saving and shows increasing impacts from cold to warm climates. The latent heat of PCM has a comparable impact (14.8-22.9%) on the annual energy saving with thermal mass. In other words, the effects of thermal mass and latent heat are significant and hence PCM windows outperform a tinted window with that provides the same thermal insulation.

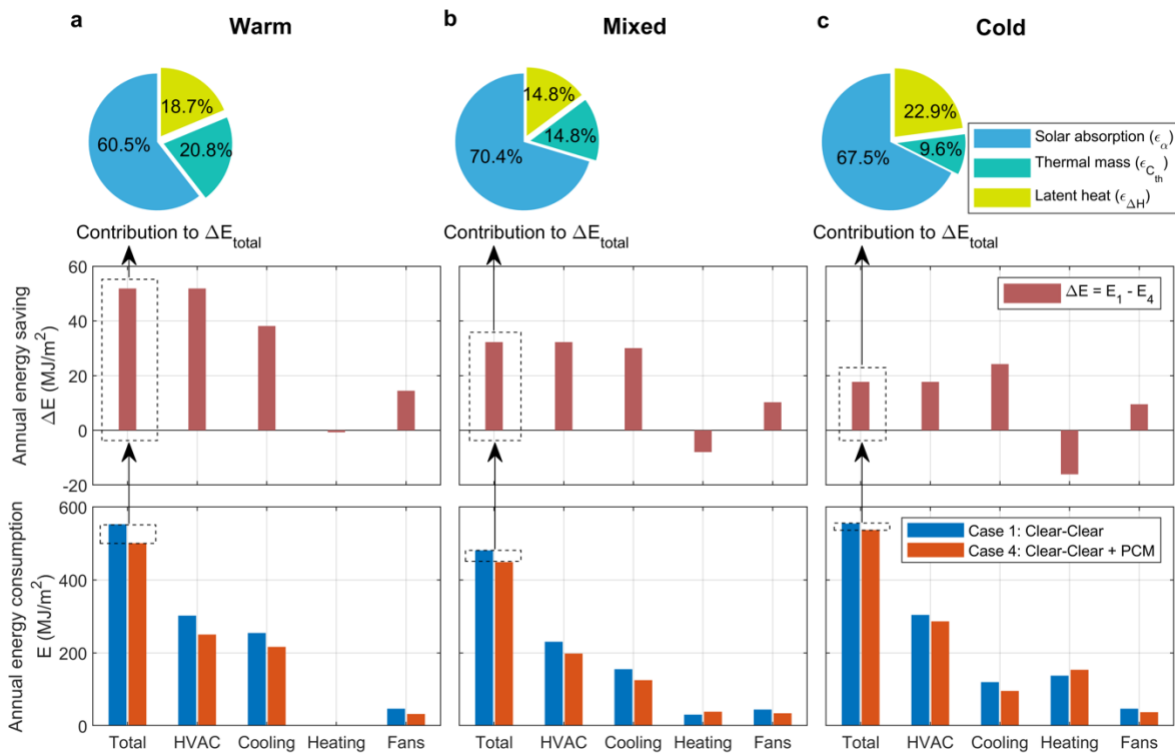


Figure 5 Bottom row: bar chart of annual energy consumption corresponding to E_1 from the Case 1 with clear-clear DPW and E_4 from the Case 4 with PCM-integrated clear-clear DPW for the total, HVAC, cooling, heating, and fans. Middle row: energy saving ΔE calculated from the bottom row ($E_1 - E_4$). Top row: pie chart of energy saving ΔE_{total} contribution from the PCM solar absorption, thermal mass, and latent heat. Each column corresponds to the results under **a.** warm, **b.** mixed, and **c.** cold climates.

3.2 Sensitivity analysis of PCM properties

To better guide the material design, we analyze the sensitivity of the annual energy savings (ΔE_{total}) to PCM properties. Unlike the logarithmic derivative used in thermal science [70], we calculate the percentage change of ΔE_{total} when a PCM property is decreased or increased by 10% from the optimal values in Table 5. Note that we fixed T_c at 36°C for all the climates. As shown in Figure 6, the energy saving is most sensitive to the solar absorptance (α_{tPCM}) of PCM for all three climates compared with other parameters. The same sign of ΔE_{total} sensitivity with the change of α_{tPCM} indicates that a higher α_{tPCM} is beneficial for overall energy savings. This is consistent with the pie chart in Figure 5 and can be understood from the point that the energy saving is dominated by reducing the cooling energy. A high solar absorptance of the window can reduce the solar heating of the room in the summer and hence reduce the cooling load in general because part of the solar heat absorbed by the window can be directly released to the exterior, thus reducing the amount of heat that needs to be removed from the space by the HVAC system.

The $\pm 10\%$ change in latent heat (ΔH) barely impacts ΔE_{total} in the warm climate but leads to about a considerable $\pm 2\%$ to $\pm 3\%$ change of ΔE_{total} in the mixed and cold climates. It can also be seen that a higher value of ΔH of the PCM is beneficial for energy saving. This indicates that TES of PCM in windows is effective for energy saving similar to the application of PCMs in opaque building envelopes, i.e., shifting the thermal energy exchange process of the building to reduce the cooling load (details will be discussed in Figure 12). The sensitivities of ΔE_{total} to c_p and k increase from warm to cold climates and are all relatively small. For T_c and ΔT_{pc} , we use the unit of temperature on the Celsius scale instead of Kelvin. For all the three climates, the base T_c is set at 36°C, which is the average of the maximum (42°C) and minimum (30°C) optimal T_c among the three climates as will be shown in Table 5. In the warm climate, T_c accounts for the second largest sensitivity after α_{tPCM} . The optimal ΔT_{pc} is 2°C for all the three climates and, therefore, the 10% change, i.e., $\pm 0.2^\circ\text{C}$, has very small impact on the change of ΔE_{total} since this is a small range even when compared with the daily temperature swing.

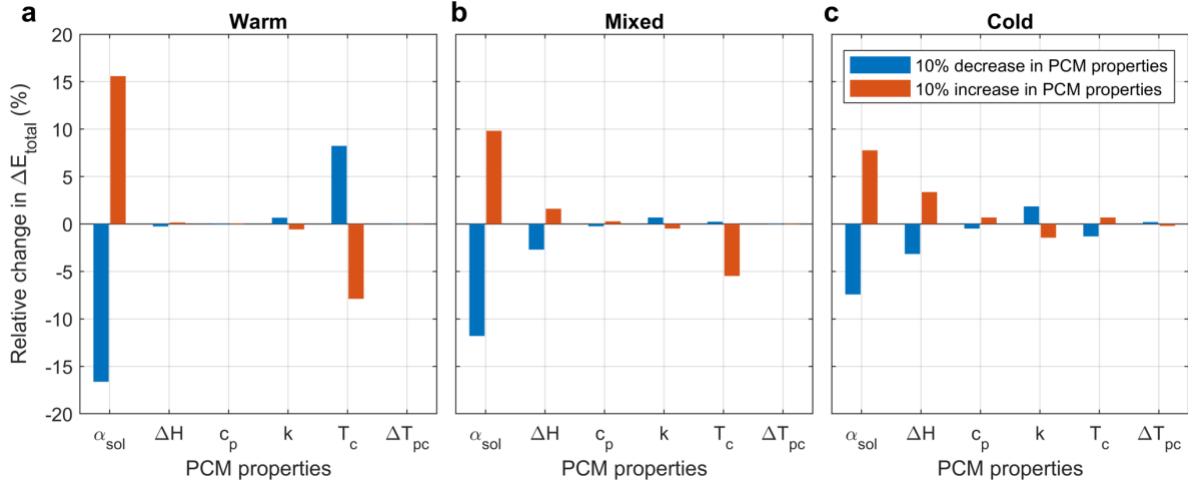


Figure 6 Sensitivity of energy saving to PCM properties that are increased or decreased by 10%, including solar absorptance (α_{PCM}), latent heat (ΔH), specific heat capacity (c_p), thermal conductivity (k), central phase change temperature (T_c) and temperature breadth of phase change (ΔT_{pc}) under **a.** warm, **b.** mixed, and **c.** cold climates. Note that here we use the unit of temperature on the Celsius scale. PCM properties are decreased or increased from the optimal values, except that the base T_c is 36°C for all the climates.

3.3 Summary statistics of six PCM variables

In the preliminary batch simulation, 972 combinations of PCM variables result in 2916 EnergyPlus runs for three climates. The total running time is around 34 hours using a computer with Intel i7 CPU and 8 logical processors. Energy differences ΔE_{total} from the preliminary simulation batch are obtained by comparing the $E_{total,4}$ in each calculation with $E_{total,1}$ in Case 1. The statistical results are shown in the form of 18 box plots in Figure 7 for the 3 climates (columns) and 6 variables (rows). In each box plot, the red central mark on each box indicates the median, and the bottom and top edges of the box indicate the 25th and 75th percentiles, respectively (the interquartile range). The short black marks above and below each box indicate the maximum and minimum, respectively.

By comparing the plots in each row in Figure 7, it can be seen that PCM windows save more energy in the warm climate than the other two. Looking at each column for a certain climate, we can draw an important conclusion that increasing the solar absorptance (α_{tPCM}) is the most efficient way to increase the annual energy saving (ΔE_{total}) for the 3 mm PCM within the scope of the material properties studied here. The strong influence of the α_{tPCM} and an increasing trend of energy saving ΔE_{total} with increasing α_{tPCM} are consistent with the observation in the sensitivity analysis. Though increasing α_{tPCM} to above 0.5 will further increase ΔE_{total} , it will decrease the visible transmittance of the window and consequently reduce the daylight and window visibility beyond a desirable level. Therefore, the optimal α_{tPCM} in this study is set at 0.5 for all the three climates.

Summary statistics of ΔE_{total} vs. PCM variables (972 combinations)

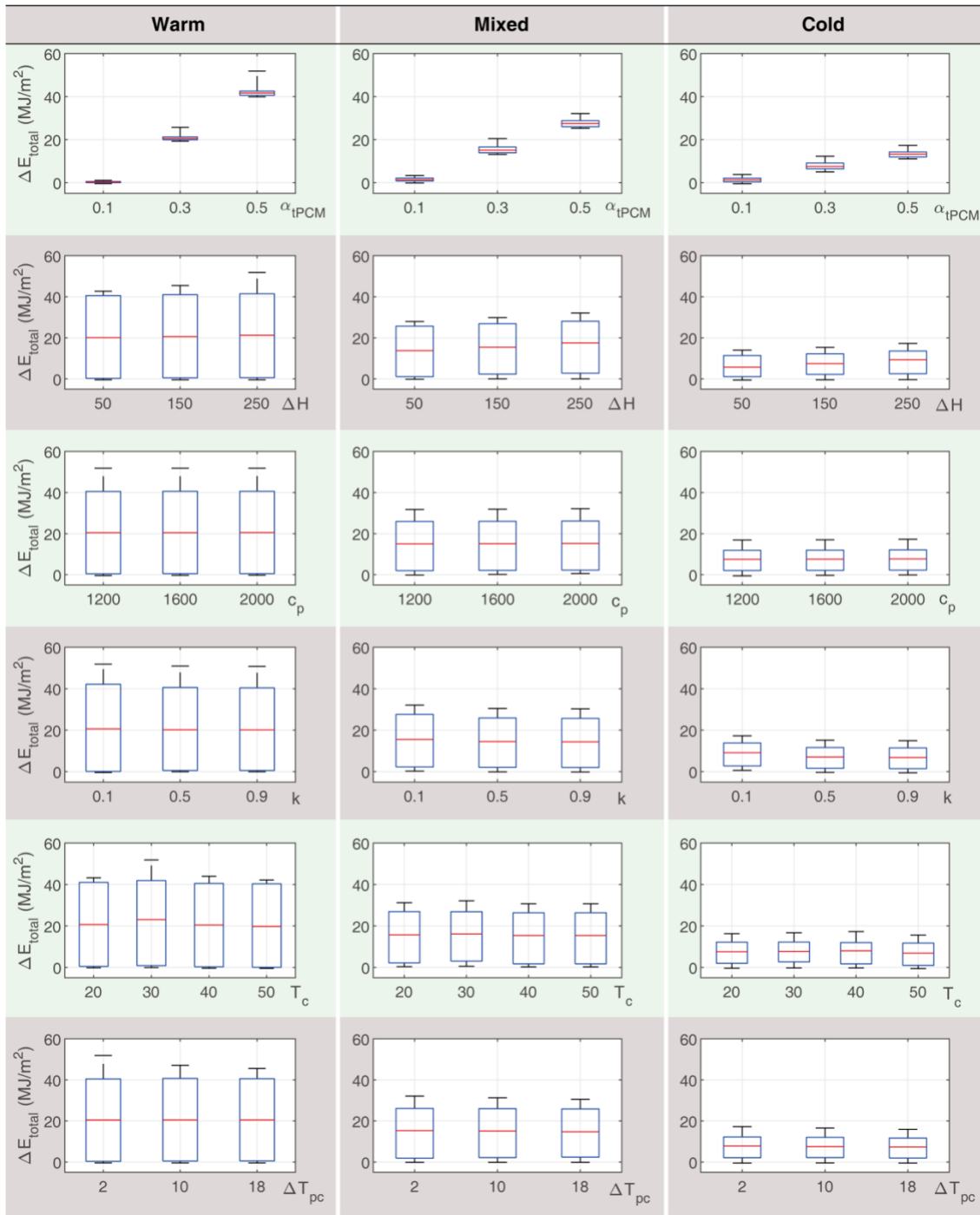


Figure 7 Statistical summary of the parametric study of energy saving per conditioned floor area of 972 combinations of six PCM properties (α_{tPCM} , ΔH , c_p , k , T_c , and ΔT_{pc}) under warm, mixed, and cold climates. In each box plot, the red central mark on each box indicates the median, and the bottom and top edges of the box indicate the 25th and 75th percentiles, respectively (the interquartile range). The short black marks above and below each box indicate the maximum and minimum, respectively.

In Figure 7, the impacts of other variables on ΔE_{total} are not as obvious as α_{tPCM} , especially with identical y-axis scale due to that large span of the data induced by changing α_{tPCM} . To better observe the maximum ΔE_{total} of the other five variables, extra statistic box plots of 324 combinations ($\alpha_{tPCM} = 0.5$) are presented in Figure 8. The top mark determines the optimal value of PCM variables. The data in the figure indicate that higher latent heat (ΔH), lower thermal conductivity (k) and lower temperature breadth of phase change (ΔT_{pc}) result in higher ΔE_{total} . These trends are consistent with the sensitivity analysis. Firstly, a higher ΔH will increase the TES density in PCM windows and can reduce the cooling energy (see discussion for Figure 12). Secondly, since windows usually have a much lower thermal resistance than walls, a lower PCM conductivity will increase the window thermal resistance and reduce the cooling power loss to the outdoor environment and hence save cooling energy. Although a low k value will reduce the heat conduction rate inside the PCM, the small thickness of the PCM, 3 mm, should compensate that to a certain extent, preventing partial transition. In fact, our simulations confirmed that the trend for k does not invert even for a PCM thickness of 18 mm, indicating that the improvement of thermal insulation dominates the ΔH loss from potential partial phase transition. A small ΔT_{pc} facilitates the phase transition in the daily cycles while a large ΔT_{pc} may cause partial phase transition and limit the effective ΔH that contributes to TES. Thus ΔE_{total} decreases with increasing ΔT_{pc} which is consistent with the results from prior small scale simulation on the surface temperature effect of adding PCM in DGU [32]. The difference in ΔE_{total} between different values of the specific heat capacity (c_p) is subtle and difficult to observe in Figure 8. To determine the optimal c_p , the top five best-performing PCMs for different climates among 972 combinations are listed in Table 4. We select an optimal c_p is 2000 J/(kg K) for all the three climates.

Regarding the central phase change temperature (T_c), ΔE_{total} shows distinct non-monotonic trends for different climates. In this preliminary batch simulation, the optimal T_c is 30°C, 30°C, and 40°C for warm, mixed, and cold climates, respectively. Finer steps (1°C) was later applied in a secondary simulation batch in order to find the optimal T_c for each climate. We confirm that an iterative optimization of the variables is not necessary since the trends for parameters other than T_c are all monotonic with the corresponding ranges limited by realistic PCM properties (e.g., ΔH can hardly increase beyond 250 kJ/kg). Thus, the optimal values for the rest five parameters are always those identified in Figure 7 for a 3 mm PCM.

Note that ΔE_{total} could be negative if the PCM properties were chosen improperly. The worst five PCMs for different climates among 972 combinations are listed in Supplementary Table 9. It is safe to conclude that low α_{tPCM} , ΔH , and c_p are adverse settings for PCM windows in terms of ΔE_{total} . The full list of the performance ranking of 972 PCMs for each climate can be found in the Supplementary Information.

Summary statistics of ΔE_{total} vs. PCM variables (324 combinations)

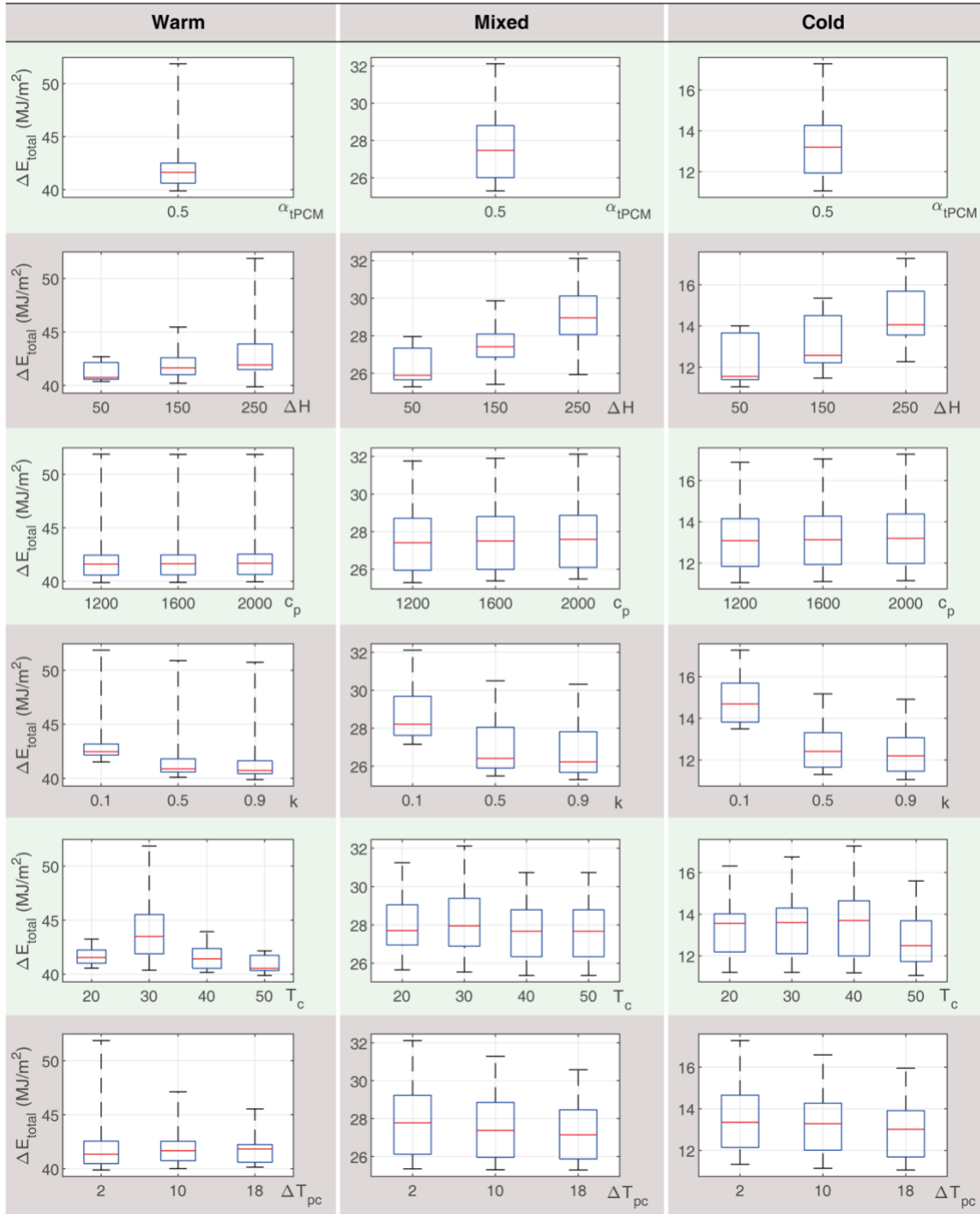


Figure 8 Statistical summary of the parametric study of energy saving per conditioned floor area of 324 combinations of six PCM properties (α_{tPCM} , ΔH , c_p , k , T_c , and ΔT_{pc}) under warm, mixed, and cold climates with α_{tPCM} fixed at 0.5. In each box plot, the red central mark on each box indicates the median, and the bottom and top edges of the box indicate the 25th and 75th percentiles, respectively (the interquartile range). The short black marks above and below each box indicate the maximum and minimum, respectively.

Table 4 Top five performance among 972 combinations

Climate types	ΔE_{total} (MJ/m ²)	PCM properties					
		α_{tPCM}	ΔH (kJ/kg)	c_p (J/(kg K))	k (W/(m K))	T_c (°C)	ΔT_{pc} (°C)
Warm	51.86	0.5	250	2000	0.1	30	2
	51.86	0.5	250	1600	0.1	30	2
	51.86	0.5	250	1200	0.1	30	2
	50.91	0.5	250	1600	0.5	30	2
	50.91	0.5	250	1200	0.5	30	2
Mixed	32.12	0.5	250	2000	0.1	30	2
	31.90	0.5	250	1600	0.1	30	2
	31.79	0.5	250	1200	0.1	30	2
	31.28	0.5	250	2000	0.1	20	2
	31.28	0.5	250	2000	0.1	30	10
Cold	17.27	0.5	250	2000	0.1	40	2
	17.04	0.5	250	1600	0.1	40	2
	16.88	0.5	250	1200	0.1	40	2
	16.76	0.5	250	2000	0.1	30	2
	16.65	0.5	250	1600	0.1	30	2

3.4 Optimal central phase change temperature (T_c)

In Figure 8, the optimal T_c varies with climate. But the steps between values of T_c are too large to identify the best values. To obtain more accurate optimal T_c for PCM windows, we run a secondary simulation batch by varying T_c from 20°C to 50°C with 1°C step (extra 27 PCMs). By fixing the other five PCM variables at their optimal values, the running time of the secondary simulation batch is around one hour using the same computer as the preliminary simulation batch. Figure 9a-c shows the annual cooling energy saving ($\Delta E_{cooling}$), heating energy saving ($\Delta E_{heating}$), and fans energy saving (ΔE_{fans}) under three climates. The total site energy saving (ΔE_{total}), which equals the sum of the three aforementioned energy savings, is shown in Figure 9d-f. The maximum ΔE_{total} corresponds with the optimal T_c , which is 30°C, 32°C, and 42°C for warm, mixed, and cold climates, respectively. In the warm climate, ΔE_{total} changes as much as about 10 MJ/m² from the best to the worst T_c . Such changes are lower in the other two climates (about 4 MJ/m² and 2 MJ/m² for mixed and cold climates, respectively). This observation is consistent with the conclusion in the sensitivity analysis. In the warm and cold climates, $\Delta E_{cooling}$ shows similar a trend to ΔE_{total} and the optimal T_c is the same as the peak temperature of cooling energy saving. In the mixed climate, however, the optimal T_c is affected by both heating and cooling energy but the peak energy saving is nearly the same as the energy saving at the optimal temperature for cooling. Hereinafter, we will focus on how T_c influences $\Delta E_{cooling}$ in the following analysis.

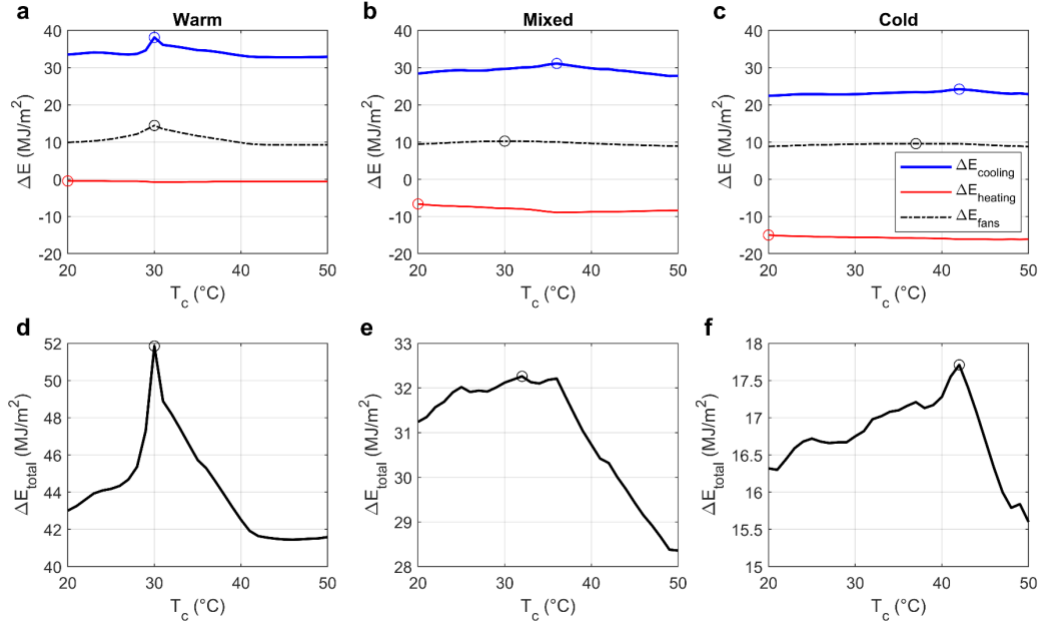


Figure 9 Energy saving vs. central phase change temperature under **a, d.** warm, **b, e.** mixed, and **c, f.** cold climates. Note that the cooling loads (summer months) dominate the energy savings. The optimal T_c s stay valid when the range of T_c is extended to -10 to 50°C (see Supplementary Figure 9).

Based on the results of the preliminary and secondary batch simulation, the optimal properties of PCM windows are obtained as listed in Table 5. Except for T_c , the optimal properties are the same for all the three climates. PCM windows benefit warm (cooling-dominated) climates more than others in reducing the total site energy use. Please note that in cold climates, the inclusion of PCMs increases the heating load ($E_{heating}$); and the energy savings are mainly due to the decrease in cooling load ($E_{cooling}$). Our simulation thus provides guidance for future materials design for PCM windows applications in different climate zones based on S-S PCMs. For DGU with common S-L PCMs with the same thickness and thermal properties but a high transmission (hence small α_{tPCM}) in the high temperature liquid state, the energy saving should be less than the results in Figure 5 considering the trend in Figure 7.

Table 5 Optimal properties of PCM windows among 999 types of PCMs for three climates

Climate types	ΔE_{total} (MJ/m ²)	PCM properties					
		α_{tPCM}	ΔH (kJ/kg)	c_p (J/(kg K))	k (W/(m K))	T_c (°C)	ΔT_{pc} (°C)
Warm	51.9	0.5	250	2000	0.1	30	2
Mixed	32.3	0.5	250	2000	0.1	32	2
Cold	17.7	0.5	250	2000	0.1	42	2

There are several factors that could influence the thermal behavior and energy savings of PCM windows. The main exterior factors include outdoor temperature and solar radiation. The main interior factor is the indoor air temperature, which is mostly determined by the heating and cooling schedules of the building. The PCM window properties are also critical to the thermal behavior. We explore these factors to understand the trend in the optimal T_c among different climate zones.

Firstly, we analyze how factors related to exterior environment impact the temperature of PCM windows. Annual summary statistics are shown in Figure 10 in the form of violin plots. In each violin plot, the central part is similar to the box plot, with the addition of a rotated kernel density plot on each side. The hollow circle mark on each solid box indicates the median, and the bottom and top edges of the solid box indicate the 25th and 75th percentiles, respectively (the interquartile range). The top and bottom ends of the line through each box indicate the maximum and minimum, respectively. The symmetrical curves outside the box plot show the probability density of the y-axis data, smoothed by a kernel density estimator.

Compared with warm climate, though cold climate shows lower median and maximum outdoor temperature (Figure 10a), the solar radiation on the PCM surface is higher because of lower solar altitude angles in cold climates, which tend to be associated with higher latitudes (Figure 10b). Consequently, the combination of the exterior factors could lead to higher PCM temperatures in the cold climate than that in the warm climate. To exclude the interference from intrinsic PCM factors (mainly T_c), here we explore the outer surface temperature of the material layer with thermal mass without latent heat in Case 3 instead of the PCM in Case 4. As shown in Figure 10c, there are higher possibilities for the temperature of this material layer to exceed 30°C during cooling hours in the cold climate than in the warm climate. This could partially explain why the optimal T_c in the cold climate is higher than that in the warm climate since high temperatures during hot days impact the cooling load most and cooling dominates the energy savings.

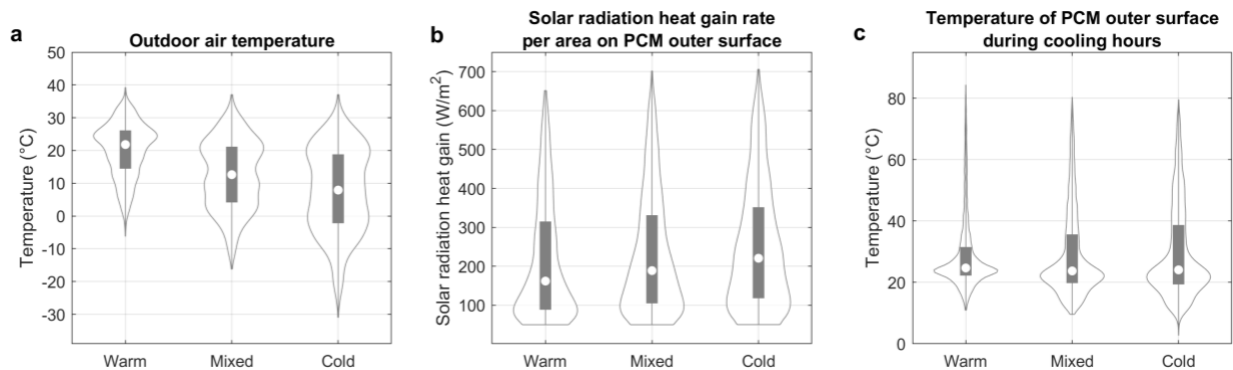


Figure 10 Annual summary statistics of **a.** outdoor air temperature, **b.** solar radiation heat gain rate per area above 50 W/m² on PCM outer surface ($\alpha_{tPCM} = 0.5$), and **c.** outer surface temperature of the material layer with thermal mass without latent heat (Case 3) during cooling hours under warm, mixed and cold climates. In each violin plot, the central part is similar to the box plot, with the addition of a rotated kernel density plot on each side. The hollow circle mark on each solid box indicates the median,

and the bottom and top edges of the solid box indicate the 25th and 75th percentiles, respectively (the interquartile range). The top and bottom ends of the line through each box indicate the maximum and minimum, respectively. The symmetrical curves outside the box plot show the probability density of the y-axis data, smoothed by a kernel density estimator.

Since the heating and cooling schedules are the same for the three climates, we will not discuss here factors related to indoor environmental conditions. A brief discussion will be introduced later regarding the influence of cooling schedule on the optimal T_c .

The statistic violin plots in Supplementary Figure 10 illustrate how T_c affects the distribution of PCM inner surface temperature, which could further influence the indoor temperature, and consequently influence the heating and cooling loads. The heat exchange between the PCM inner surface and indoor air can be described by the heat flux through that interface (in W/m^2). The energy released from the PCM window to the room can be calculated by integrating heat flux over time, then multiplying by the PCM area. The effects of PCM energy release on building energy saving are twofold. When the HVAC system is in cooling mode, less energy release from PCM to the room would benefit the energy saving. On the other hand, when the HVAC system is in the heating mode, the positive PCM energy release could be a bonus to heating energy savings. Therefore, we calculate the PCM energy release to the room in non-heating hours over a year using various T_c . The results shown in Figure 11 indicate that the T_c with low PCM energy release is consistent with the optimal T_c for cooling energy saving in Figure 9a-c for the three climates. Thus, we can conclude that the optimal PCM windows regulate the cooling loads by releasing less energy to the room during cooling time in the warm and cold climates. For the mixed climate, however, the optimal T_c (32°C) is different from the temperature for the maximum cooling energy saving and minimum energy release (36°C) because it is determined by both cooling and heating energy.

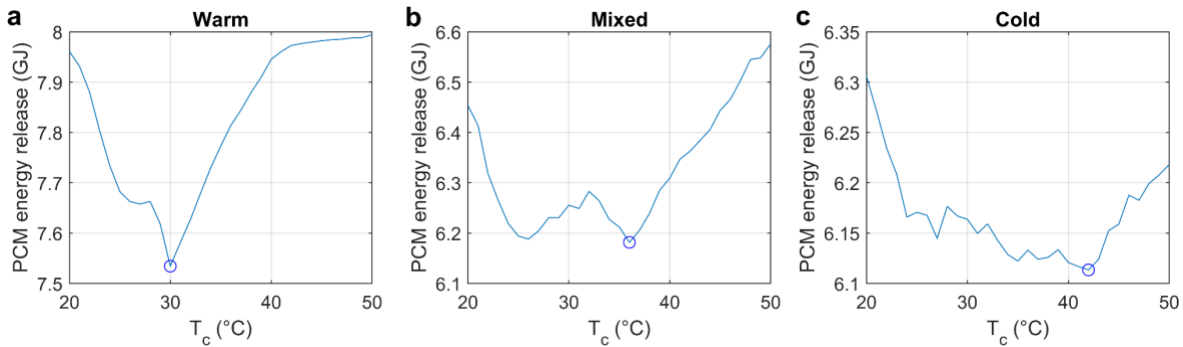


Figure 11 PCM energy release to the room during non-heating hours under **a.** warm, **b.** mixed, and **c.** cold climates.

We further explore the thermal behavior of PCM windows by zooming in the time span and focusing on three summer days, when cooling dominates, and no heating energy is required.

Figures 12a-d show the results of the PCM surface temperature, indoor and outdoor air temperature, heat flux at the inner surface of the PCM layer and the hourly cooling load for three different T_c values in the warm climate. The optimal T_c is 30°C and is marked by a bold blue line. As comparisons, results of two T_c (30±5°C) are marked with green and red lines, respectively. For PCM with $T_c = 25^\circ\text{C}$, it transitions to its high temperature state early before the simulated three days in Figure 12 and stays in this state for these three days. For the PCM with $T_c = 35^\circ\text{C}$, it barely reaches the transition temperature and does not fully “melt” and there is only a short period of time during which the phase change modulates the heat flux.

In comparison, the PCM windows with optimal T_c (30°C) have a long period of time with nearly constant PCM surface temperature as shown in Figure 12a and postpone the energy release to the room which also reduces the daily total heat flow into the room as shown in Figure 12c. It is also observed that the inclusion of PCM with optimal T_c can delay the peak in heat flux by ~5 h compared with PCM with other T_c s (Figure 12c), resulting in reduced peaks of the cooling energy in Figure 12d. Such peak shift can reduce the gap between the peak and off-peak electricity demand [71]. A lower PCM temperature during the peak hour around noon time can reduce the heat flux into the room and hence reduces the cooling load. On the other hand, a higher temperature of the PCM in off-peak hours after ~17:00 does not burden the cooling load too much (Figure 12d). This is because the outdoor temperature is relatively low during that time such that the PCM can dissipate some of the stored heat to the exterior and hence the heat flux into the room does not increase by more than the surplus during the peak hour for PCM with different T_c values. In addition, the overall building envelope and air temperature also becomes low (lower than the setpoint) after ~17:00 hence the cooling demand is low, which leads to a smaller amount of cooling power increase compared with the cases with different T_c values as shown in Figure 13d. The other two climates follow the similar manner of reducing the PCM energy release and cooling loads. Details can be found in the Supplementary Figure 11-12.

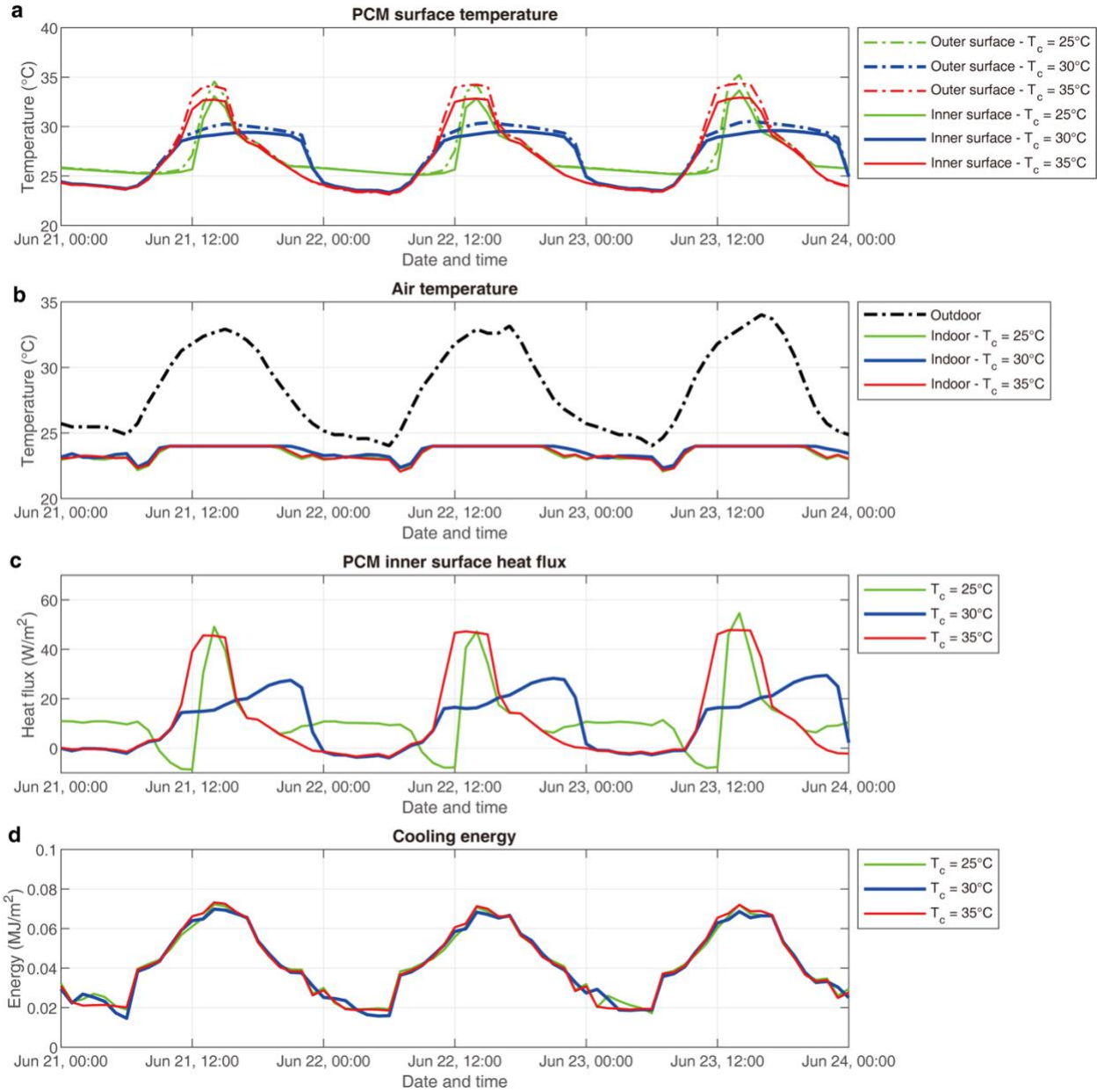


Figure 12 **a.** PCM surface temperature, **b.** indoor and outdoor temperature, **c.** heat flux of PCM inner surface (a positive heat flux means heat flows from the PCM to the room), **d.** hourly cooling energy for three summer days (June 21-23) in the warm climate case. The optimal T_c is 30°C (blue curves) and is compared with the results from the calculation where $T_c = 25^\circ\text{C}$ and 35°C (green and red curves).

3.5 Reduction of peak cooling loads with PCM windows

Buildings in warm (cooling-dominated) climates require the use of significant energy for cooling during summertime. The peak cooling loads (AC and fans) usually appear during daytime, peaking between 12:00 to 16:00 and can be a burden on the electricity grid. Figure 13 shows how PCM windows cut down the daily and hourly peak cooling loads compared with clear-clear DPW. As

can be easily seen, the peak cooling load is smaller at almost all time during the year when the PCM is incorporated. The reduction of the peak loads not only provides relief to the grid, but also can significantly reduce the costs of electricity consumption in the building, due to the fact that, for many commercial buildings, rates paid for electricity can be more impacted by peak use than the actual amount of energy used during a particular billing period.

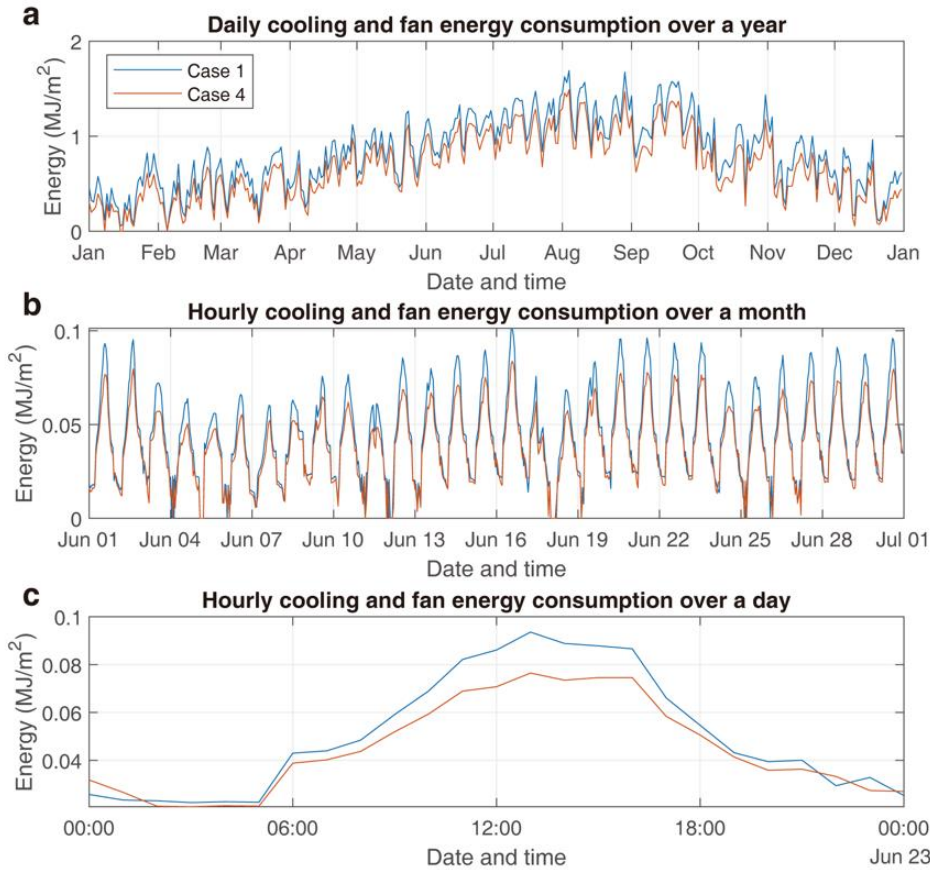


Figure 13 **a.** Daily cooling and fan energy consumption per conditioned floor area of Case 1 and 4 over the year in warm climate. **b.** Hourly cooling and fan energy consumption per conditioned floor area of Case 1 and 4 over June. **c.** Hourly cooling and fan energy consumption per conditioned floor area of Case 1 and 4 on June 23rd.

4. Discussion

4.1 Hysteresis effects of PCMs on the thermal and energy performance

In this parametric study, the hysteresis effects (supercooling) of PCMs are not considered due to the lack of a proper model of PCM in a partial “melting-freezing” cycle [69] in EnergyPlus [66]. But that does not mean the hysteresis effects are not important. In fact, such effects could reduce cooling or heating loads and further affect the optimal T_c . Here, we use one cooling-dominated day in the warm climate as an example, in which the PCM can go through a complete “melting-freezing” cycle which can be properly calculated with the current algorithm. Note that the solid-to-solid PCM is not really “melting” but transiting from a low-temperature phase to a high-

temperature phase while maintaining a solid state. However, we will still use the phrase of “melting” and “freezing” to describe the phase transitions of the PCM so that it is easy to understand by readers.

In Figure 14a-f, the left and right columns indicate a PCM with a hysteresis of 9°C (with central “melting” temperature $T_m = 30^\circ\text{C}$ and “freezing” temperature $T_f = 21^\circ\text{C}$) and a PCM without hysteresis, respectively. Four PCM states are marked in enthalpy plots in Figure 14a and b with integer numbers from -2 to +2. The red arrows indicate that the PCM is in “melting” (-1) or “melted” (-2) states; and the blue arrows indicate the PCM is in “freezing” (+1) or “frozen” (+2) states. The PCM outer and inner surface states are shown in Figure 14c and d. The inner surface state lags behind the outer surface state due to the heat diffusion process across the PCM thickness. Since the most important thermal effect of the PCM comes from the phase transition, we focus on the “freezing” (+1) and “melting” (-1) state. For both PCMs with and without hysteresis, the “melting” (-1) state of the inner surface starts and stops at almost the same time (10:41 - 13:44 for with hysteresis and 10:40 - 13:43 for without hysteresis, respectively). However, the “freezing” (+1) state of the inner surface of the PCM with hysteresis spans from 02:34 to 07:39. This is a heat releasing state that has a negative impact on energy saving since cooling is continuously demanded throughout the whole day. The “freezing” state of the inner surface of the PCM without hysteresis happens from 15:57 to 22:34, which has a longer duration than the PCM with hysteresis. Figure 14e and f show the inner and outer surface temperature of the two PCMs which are consistent with the state plot in Figure 14c and d. The difference between the temperature behaviors of the two PCMs is caused by hysteresis.

Figure 14g and h show the hourly heat flux of the PCM inner surface and cooling energy, respectively. The same as before, a positive heat flux means heat flows from the PCM to the room. By comparing the PCMs with and without hysteresis (red and blue), we notice that the PCM with hysteresis releases less energy to the room during the afternoon and nighttime since it remains in the “melted” state. Moreover, the PCM even absorbs heat from the room during the heat-releasing time when it is “freezing” since its temperature is lower than the room temperature with a setpoint of 24°C. As we can confirm with the heat flux at the outer surface, the PCM with hysteresis releases the latent heat absorbed during the daytime to the exterior during the nighttime. Consequently, by eliminating the heat release to the indoor environment by shifting the “freezing” process to late night, the PCM with hysteresis results in less cooling energy consumption (628.8 kJ/m²) than that without hysteresis (633.8kJ/m²). An extra example of PCM performance on a heating-dominated day can be found in the Supplementary Figure 13. The PCM with hysteresis also consumes less heating energy than that without hysteresis.

Although the daily energy saving in Figure 14h by hysteresis-induced load diverting effect is subtle (5.0 kJ/m²), the annual accumulated saving could be considerable. Additionally, the optimal T_c might shift if the hysteresis effects are considered for the entire year. Further research on optimizing the properties of PCM with hysteresis effects should be considered once a valid PCM model of partial “melting-freezing” cycles is available in EnergyPlus.

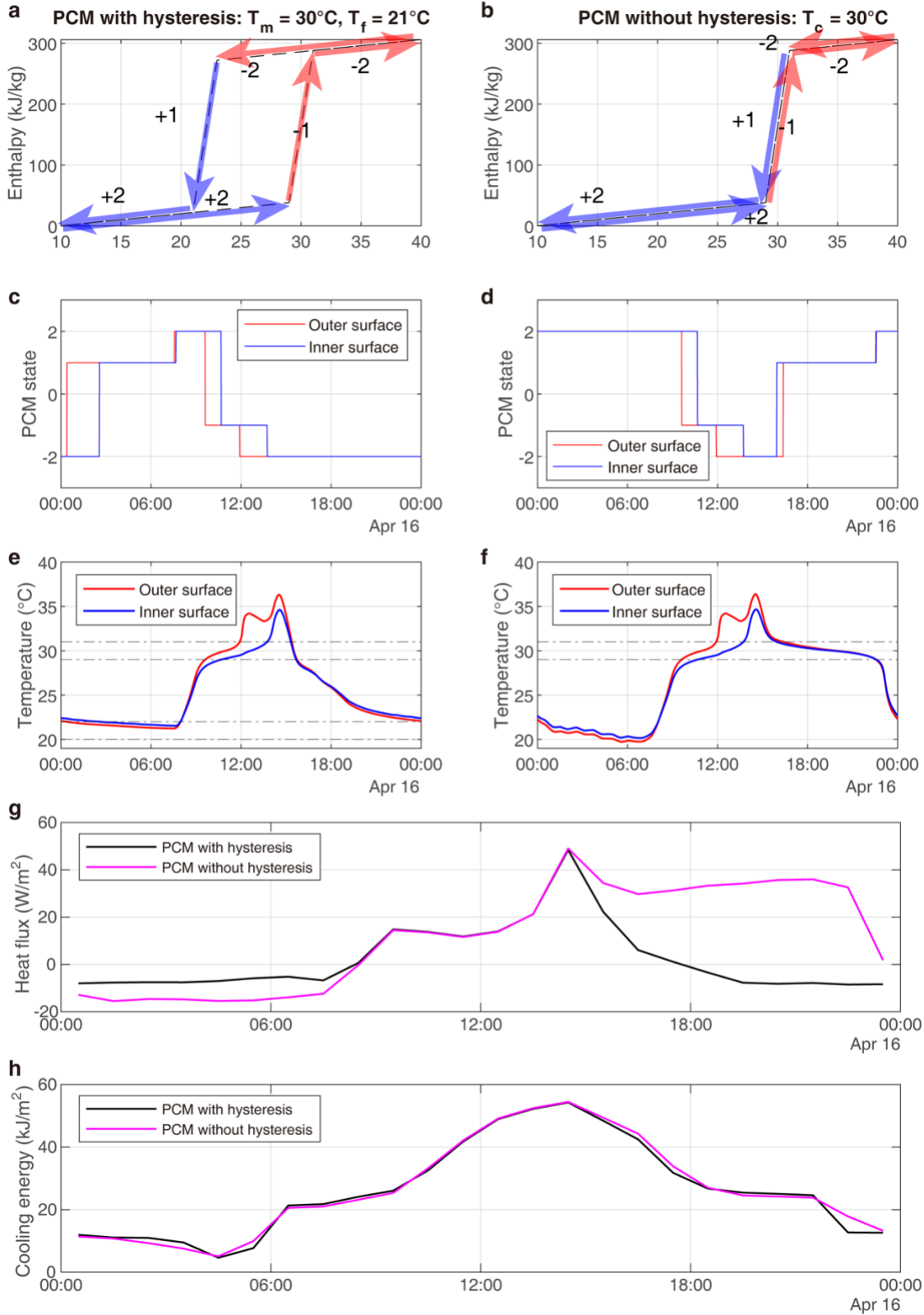


Figure 14 Comparison of the PCM state and surface temperature of PCM with and without hysteresis on April 16th, under warm climate.

4.2 Thermochromic effect of PCMs

In this study, we assume that the solid-to-solid PCMs maintain its optical features in every state. In reality, such PCMs could be designed to have thermochromic effects, i.e., the solar transmittance and absorptance could be different in different states. Although users often desire to control the visibility of their window, thermochromic windows are still welcome in certain building scenarios.

Thermochromic effects of PCMs trigger further questions, e.g., how to design the optical features of each state for different buildings and climates? How do thermochromic effects shift the optimal phase change temperature? What if the thermochromic PCMs have hysteresis effects? To answer those questions, a sophisticated model is required, which is possible to be developed based on the EnergyPlus model proposed in this study.

4.3 PCM thickness

We have kept the thickness of the PCM layer a constant (3 mm) in this parametric study. In practice, the thickness of PCM could be further adjusted to achieve more energy savings. Note that optical features of the PCM layer will also change with the PCM thickness in real cases, i.e., a thicker PCM layer might result in a less transparent window. To make a simple comparison, here we assume the optical features of the PCM layer are constants (see Table 3 and 5) when we vary the PCM thickness from 1 to 20 mm. Simulation results suggest that energy saving will increase with a thicker PCM layer. In real cases, a tradeoff has to be made between energy saving and visible transmittance of the window when we optimize the PCM thickness. Detailed simulation results can be found in Supplementary Figure 14.

4.4 Building factors that affect the optimization of PCM windows

4.4.1 Cooling temperature setpoint

As mentioned above, the building model in this study uses a standard heating schedule and a simplified cooling schedule (cooling setpoint is 24°C for all hours) for a medium commercial office. To explore the impact of cooling setpoint on the optimal T_c , we run two extra secondary batch simulations by changing the cooling setpoint from 24°C to 23°C and 25°C. Results show that the optimal T_c for warm and cold climates maintain the same (variation within 1°C). However, the optimal T_c for the mixed climate shifts from 35°C to below 30°C. A possible reason for such shifts is that both heating and cooling play an important role in the mixed climate. Detailed results can be found in the Supplementary Figure 15-16.

4.4.2 Window orientation

In this study, the PCM window is on a south-facing exterior wall. Different orientations of the PCM window will result in different levels of solar heat gain, which is an important factor that

could affect the optimal PCM properties. We first ran the preliminary simulations batch for east, west, and north facing PCM windows. We found that among the six parameters studied here four of the optimal PCM variables for different orientation are the same as that for the south case, except T_c and ΔT_{pc} . Then we use 16 orientations (22.5° step), 21 T_c values (from 0°C to 100°C with 5°C step) and 3 ΔT_{pc} values (2°C , 10°C , 18°C) as variables to run an extra batch simulation to find the optimal T_c and ΔT_{pc} for different orientations of PCM windows. Results are shown in Figure 15. The optimal T_c becomes higher when the PCM windows are facing east or west due to lower solar altitude angles. The north-facing PCM windows show the lowest optimal T_c . Those conclusions further confirmed that the level of incident solar radiation plays a key role in determining the optimal T_c . Regarding ΔT_{pc} , the optimal value is 2°C for all the orientations since a sharp transition is beneficial for the exploitation of latent heat when there is no hysteresis.

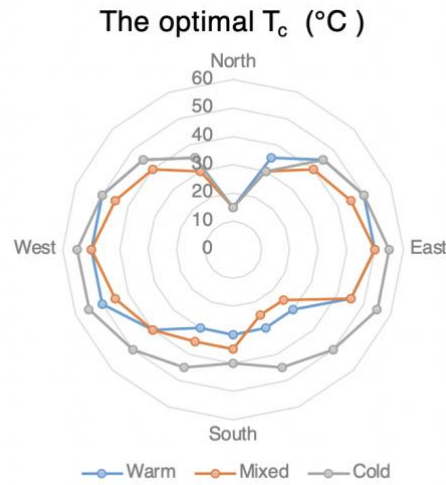


Figure 15 Radar map of the optimal T_c 16 orientations of PCM windows under three climates.

4.4.3 Interior lighting

The interior lighting consumption is fixed in this study. Therefore, theoretically the maximum ΔE_{total} could be achieved when α_{tPCM} equals 1 if visibility through the window is not a considered, which of course would make the window function like an opaque building envelope element such as a wall. In reality, in many cases interior lights can be controlled by light and motion sensors to save energy, especially in commercial buildings. In this case, increasing α_{tPCM} can increase the energy consumption with lighting due to increased need for the use of interior electric lighting. In such a case, the optimal α_{tPCM} would be a value that achieve a balance between ΔE_{HVAC} and ΔE_{lights} that maximizes ΔE_{total} . If α_{tPCM} is set to be extremely high, e.g., 0.9, then we would have to consider window visibility and constrain the optimal by the minimum acceptable visible transmittance of the window. In this study, we don't intend to consider the lighting consumption

to affect optimal PCM properties because the possible variations in interior lighting design and control strategy would introduce additional variables that would, at this stage, detract from a careful examination of the thermal behavior of the PCM window. We built new models considering daylighting and briefly discussed the daylighting issues in Supplementary Note 2.

4.5 Comparison with low-e counterparts

To compare the PCM windows with mature commercial technologies, we simulated the same building model with two low-e-clear double-pane windows, whose technical details can be found in the Supplementary Table 10. Low-e window no. 01 has a solar transmittance closed to that of the optimal PCM window. Low-e window no. 02 has a SHGC of 0.229, which is usually used for warm climates. As shown in Figure 16a, the optimal PCM windows result in comparable HVAC energy savings to the low-e counterparts. In the warm climate, PCM windows not only save more HVAC energy than low-e windows, but also are superior in flattening the peak energy load profile during summer days (Figure 16b). A detailed comparison of daily and hourly cooling and fan energy between PCM and low-e windows can be found in Supplementary Figure 17.

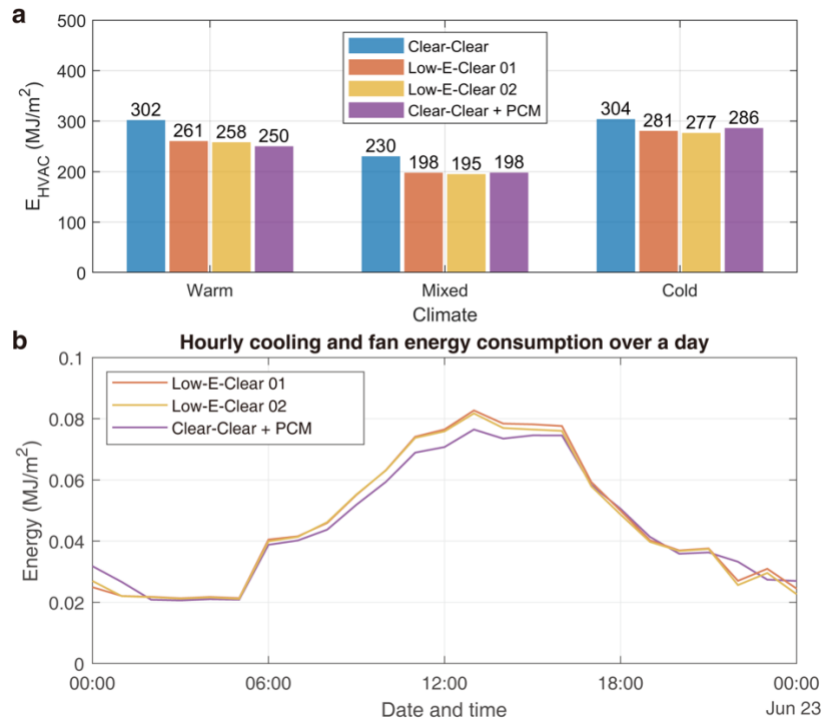


Figure 16 **a.** Annual energy consumption by HVAC per conditioned floor area using clear-clear double-pane window, low-e-clear DPW (No. 01 & 02), and clear-clear DPW integrated with PCM under warm, mixed, and cold climates. **b.** Hourly cooling and fan energy consumption using low-e-clear DPW and clear-clear DPW integrated with PCM on a summer day (June 23rd) in the warm climate.

5. Conclusion

In this work, we investigate the energy savings for commercial buildings by incorporating semi-transparent phase change material (PCM) in transparent window glazing. We circumvent EnergyPlus's (Version 9.4.0) inability to simulate translucent PCM windows by employing a thermally equivalent model. Additionally, we define four window cases to quantitatively distinguish the contribution to energy savings from solar absorption, thermal mass, and latent heat. We run batch simulations parametrically sweeping over six PCM variables, among which, higher solar absorptance (0.5), latent heat (250 kJ/kg), and specific heat capacity (2000 J/(kg K)), and lower thermal conductivity (0.1 W/(m K)) and temperature breadth of phase change (2°C) minimize building energy consumption. The optimal central phase change temperature, however, depends on the climate types, i.e., warm (30°C), mixed (32°C), and cold (42°C).

Compared with a clear-clear double-pane window, the optimal PCM windows save 9.4%, 6.7%, and 3.2% total site energy and 17.2%, 14.0%, and 5.8% HVAC energy in the warm, mixed, and cold climates, respectively. In all the three climates, solar absorption contributes to the majority of energy saving (~60%-70%). In the warm climate, where the energy saving is most obvious, thermal mass and latent heat of PCM contribute to 20.8% and 18.7% of energy saving, respectively. Among the six PCM variables, solar absorptance is the parameter to which the energy saving is most sensitive for all the three climates. The thermal behavior of PCM windows could be influenced by several extrinsic factors, such as solar radiation heat gain, indoor and outdoor temperature, etc. We demonstrated that PCM with the optimal central phase change temperature released the least heat into the room when the building's HVAC system is in cooling mode, and consequently resulted in the maximum energy saving. For the same building in the same climate, the optimal central phase change temperature varies with the orientations of PCM windows. The east and west-facing PCM windows have higher optimal central phase change temperature than the south-facing windows due to higher solar radiation heat gain. The optimal PCM windows have already revealed comparable performance with low-e windows in cooling-dominated climates. Further improving the key properties and reducing the cost could make PCM windows a promising building technology.

Reference

- [1] B. P. Center, "Annual Energy Outlook 2020," 2020.
- [2] I. E. A. and the U. N. E. P. Global Alliance for Buildings and Construction, "2019 Global status report for buildings and construction: Towards a zero-emission, efficient and resilient buildings and construction sector." UNEP Nairobi, 2019.
- [3] H. Akeiber *et al.*, "A review on phase change material (PCM) for sustainable passive cooling in building envelopes," *Renew. Sustain. Energy Rev.*, vol. 60, pp. 1470–1497, 2016.
- [4] M. Deru *et al.*, "US Department of Energy commercial reference building models of the national building stock," 2011.
- [5] L. Pérez-Lombard, J. Ortiz, and C. Pout, "A review on buildings energy consumption information," *Energy Build.*, vol. 40, no. 3, pp. 394–398, 2008.
- [6] Z. J. Zhai and J. M. Helman, "Implications of climate changes to building energy and design,"

- Sustain. Cities Soc.*, vol. 44, pp. 511–519, 2019.
- [7] M. Saffari, A. de Gracia, S. Ushak, and L. F. Cabeza, “Economic impact of integrating PCM as passive system in buildings using Fanger comfort model,” *Energy Build.*, vol. 112, pp. 159–172, 2016.
- [8] P. Marin *et al.*, “Energy savings due to the use of PCM for relocatable lightweight buildings passive heating and cooling in different weather conditions,” *Energy Build.*, vol. 129, pp. 274–283, 2016.
- [9] J. Kośny, *PCM-enhanced building components: an application of phase change materials in building envelopes and internal structures*. Springer, 2015.
- [10] F. Guarino *et al.*, “PCM thermal energy storage in buildings: experimental study and applications,” *Energy Procedia*, vol. 70, pp. 219–228, 2015.
- [11] T. Abergel, J. Dulac, I. Hamilton, M. Jordan, and A. Pradeep, “Global Status Report for Buildings and Construction-towards a zero-emissions, efficient and resilient buildings and construction sector,” 2019.
- [12] K. Muruganantham, P. Phelan, P. Horwath, D. Ludlam, and T. McDonald, “Experimental investigation of a bio-based phase change material to improve building energy performance,” in *Energy Sustainability*, 2010, vol. 43949, pp. 979–984.
- [13] K. O. Lee, M. A. Medina, E. Raith, and X. Sun, “Assessing the integration of a thin phase change material (PCM) layer in a residential building wall for heat transfer reduction and management,” *Appl. Energy*, vol. 137, pp. 699–706, 2015.
- [14] L. Karim, F. Barbeon, P. Gegout, A. Bontemps, and L. Royon, “New phase-change material components for thermal management of the light weight envelope of buildings,” *Energy Build.*, vol. 68, pp. 703–706, 2014.
- [15] M. J. Abden, Z. Tao, Z. Pan, L. George, and R. Wuhrer, “Inclusion of methyl stearate/diatomite composite in gypsum board ceiling for building energy conservation,” *Appl. Energy*, vol. 259, p. 114113, 2020.
- [16] C. Li *et al.*, “Experimental thermal performance of wallboard with hybrid microencapsulated phase change materials for building application,” *J. Build. Eng.*, vol. 28, p. 101051, 2020.
- [17] N. Soares, A. R. Gaspar, P. Santos, and J. J. Costa, “Multi-dimensional optimization of the incorporation of PCM-drywalls in lightweight steel-framed residential buildings in different climates,” *Energy Build.*, vol. 70, pp. 411–421, 2014.
- [18] J. Hu and X. Yu, “Thermo and light-responsive building envelope: energy analysis under different climate conditions,” *Sol. Energy*, vol. 193, pp. 866–877, 2019.
- [19] M. Saffari, A. de Gracia, S. Ushak, and L. F. Cabeza, “Passive cooling of buildings with phase change materials using whole-building energy simulation tools: A review,” *Renew. Sustain. Energy Rev.*, vol. 80, pp. 1239–1255, 2017.
- [20] Q. Al-Yasiri and M. Szabó, “Incorporation of phase change materials into building envelope for thermal comfort and energy saving: A comprehensive analysis,” *J. Build. Eng.*, p. 102122, 2020.
- [21] L. F. Cabeza, A. Castell, C. de Barreneche, A. De Gracia, and A. I. Fernández, “Materials used as PCM in thermal energy storage in buildings: A review,” *Renew. Sustain. Energy Rev.*, vol. 15, no. 3, pp. 1675–1695, 2011.
- [22] I. Vigna, L. Bianco, F. Goia, and V. Serra, “Phase change materials in transparent building envelopes: A Strengths, Weakness, Opportunities and Threats (SWOT) analysis,” *Energies*, vol. 11, no. 1, p. 111, 2018.
- [23] P. A. Fokaides, A. Kylili, and S. A. Kalogirou, “Phase change materials (PCMs) integrated into transparent building elements: a review,” *Mater. Renew. Sustain. energy*, vol. 4, no. 2, p. 6, 2015.
- [24] M. Aburas, V. Soebarto, T. Williamson, R. Liang, H. Ebendorff-Heidepriem, and Y. Wu, “Thermochromic smart window technologies for building application: A review,” *Appl. Energy*, vol. 255, p. 113522, 2019.
- [25] R. Baetens, B. P. Jelle, and A. Gustavsen, “Properties, requirements and possibilities of smart windows for dynamic daylight and solar energy control in buildings: A state-of-the-art review,”

- Sol. energy Mater. Sol. cells*, vol. 94, no. 2, pp. 87–105, 2010.
- [26] Y. Zhou *et al.*, “Liquid Thermo-Responsive Smart Window Derived from Hydrogel,” *Joule*, vol. 4, no. 11, pp. 2458–2474, 2020.
- [27] S. Grynning, F. Goia, E. Rognvik, and B. Time, “Possibilities for characterization of a PCM window system using large scale measurements,” *Int. J. Sustain. Built Environ.*, vol. 2, no. 1, pp. 56–64, 2013.
- [28] B. Sun *et al.*, “Multibandgap quantum dot ensembles for solar-matched infrared energy harvesting,” *Nat. Commun.*, vol. 9, no. 1, p. 4003, 2018.
- [29] D. Li, Z. Li, Y. Zheng, C. Liu, A. K. Hussein, and X. Liu, “Thermal performance of a PCM-filled double-glazing unit with different thermophysical parameters of PCM,” *Sol. energy*, vol. 133, pp. 207–220, 2016.
- [30] B. Durakovic and M. Torlak, “Experimental and numerical study of a PCM window model as a thermal energy storage unit,” *Int. J. Low-Carbon Technol.*, vol. 12, no. 3, pp. 272–280, 2017.
- [31] B. Duraković and S. Mešetović, “Thermal performances of glazed energy storage systems with various storage materials: An experimental study,” *Sustain. Cities Soc.*, vol. 45, pp. 422–430, 2019.
- [32] K. Zhong, S. Li, G. Sun, S. Li, and X. Zhang, “Simulation study on dynamic heat transfer performance of PCM-filled glass window with different thermophysical parameters of phase change material,” *Energy Build.*, vol. 106, pp. 87–95, 2015.
- [33] P. Dellicompagni, J. Franco, D. Heim, and A. Wieprzkowicz, “Numerical modeling of phase change materials using simusol software,” *Appl. Therm. Eng.*, vol. 170, p. 114772, 2020.
- [34] F. Goia, “Thermo-physical behaviour and energy performance assessment of PCM glazing system configurations: A numerical analysis,” *Front. Archit. Res.*, vol. 1, no. 4, pp. 341–347, 2012.
- [35] F. Goia, M. Perino, and V. Serra, “Experimental analysis of the energy performance of a full-scale PCM glazing prototype,” *Sol. Energy*, vol. 100, pp. 217–233, 2014.
- [36] F. Goia, L. Bianco, Y. Cascone, M. Perino, and V. Serra, “Experimental analysis of an advanced dynamic glazing prototype integrating PCM and thermotropic layers,” *Energy Procedia*, vol. 48, pp. 1272–1281, 2014.
- [37] L. Bianco, Y. Cascone, F. Goia, M. Perino, and V. Serra, “Responsive glazing systems: Characterisation methods and winter performance,” *Sol. Energy*, vol. 155, pp. 372–387, 2017.
- [38] Y. Hu, R. Guo, and P. K. Heiselberg, “Performance and control strategy development of a PCM enhanced ventilated window system by a combined experimental and numerical study,” *Renew. Energy*, vol. 155, pp. 134–152, 2020.
- [39] D. Li, B. Wang, Q. Li, C. Liu, M. Arıcı, and Y. Wu, “A numerical model to investigate non-gray photothermal characteristics of paraffin-containing glazed windows,” *Sol. Energy*, vol. 194, pp. 225–238, 2019.
- [40] M. Ahmed, A. Radwan, A. Serageldin, S. Memon, T. Katsura, and K. Nagano, “Thermal Analysis of a New Sliding Smart Window Integrated with Vacuum Insulation, Photovoltaic, and Phase Change Material,” *Sustainability*, vol. 12, no. 19, p. 7846, 2020.
- [41] D. Bionda, P. Kräuchi, I. Plüss, and M. Schröcker, “Simulation of the thermal performance of translucent phase change materials and whole-building energy implications,” no. March 2016, pp. 673–680, 2015.
- [42] D. Bionda, P. Kräuchi, I. Plüss, and M. Schröcker, “Building energy simulation of the thermal performance of translucent PCM exposed to different climates.”
- [43] Y. Wang, B. Wu, Y. Zhao, Q. Liu, and J. Lei, “Study on a novel solid–solid phase change materials: solvent-free preparation, thermal properties and phase separation behaviors,” *J. Therm. Anal. Calorim.*, vol. 141, no. 4, pp. 1305–1315, 2020.
- [44] A. Sivanathan *et al.*, “Phase change materials for building construction: An overview of nano-/micro-encapsulation,” *Nanotechnol. Rev.*, vol. 9, no. 1, pp. 896–921, 2020.
- [45] C. R. Raj, S. Suresh, R. R. Bhavsar, and V. K. Singh, “Recent developments in thermo-physical property enhancement and applications of solid solid phase change materials,” *J. Therm. Anal.*

- Calorim.*, vol. 139, no. 5, pp. 3023–3049, 2020.
- [46] K. Pielichowska and K. Pielichowski, “Phase change materials for thermal energy storage,” *Prog. Mater. Sci.*, vol. 65, pp. 67–123, 2014.
- [47] P. J. Shamberger, “Cooling capacity figure of merit for phase change materials,” *J. Heat Transfer*, vol. 138, no. 2, 2016.
- [48] L. Fan and J. M. Khodadadi, “Thermal conductivity enhancement of phase change materials for thermal energy storage: a review,” *Renew. Sustain. Energy Rev.*, vol. 15, no. 1, pp. 24–46, 2011.
- [49] M. H. Abokersh, M. Osman, O. El-Baz, M. El-Morsi, and O. Sharaf, “Review of the phase change material (PCM) usage for solar domestic water heating systems (SDWHS),” *Int. J. Energy Res.*, vol. 42, no. 2, pp. 329–357, 2018.
- [50] H. Manz, P. W. Egolf, P. Suter, and A. Goetzberger, “TIM–PCM external wall system for solar space heating and daylighting,” *Sol. Energy*, vol. 61, no. 6, pp. 369–379, 1997.
- [51] P. Mishra, K. Stockmal, G. Ardito, M. Tao, S. Van Dessel, and S. Granados-Focil, “Thermooptically responsive phase change materials for passive temperature regulation,” *Sol. Energy*, vol. 197, no. August 2019, pp. 222–228, 2020.
- [52] J. Peng, L. Lu, and M. Wang, “A new model to evaluate solar spectrum impacts on the short circuit current of solar photovoltaic modules,” *Energy*, vol. 169, pp. 29–37, 2019.
- [53] Z. Wang *et al.*, “Dynamic tuning of optical absorbers for accelerated solar-thermal energy storage,” *Nat. Commun.*, vol. 8, no. 1, pp. 1–9, 2017.
- [54] M. Chen, Y. He, Q. Ye, Z. Zhang, and Y. Hu, “Solar thermal conversion and thermal energy storage of CuO/Paraffin phase change composites,” *Int. J. Heat Mass Transf.*, vol. 130, pp. 1133–1140, 2019.
- [55] T. Silva, R. Vicente, C. Amaral, and A. Figueiredo, “Thermal performance of a window shutter containing PCM: Numerical validation and experimental analysis,” *Appl. Energy*, vol. 179, pp. 64–84, 2016.
- [56] S. Drissi, T.-C. Ling, K. H. Mo, and A. Eddhahak, “A review of microencapsulated and composite phase change materials: Alteration of strength and thermal properties of cement-based materials,” *Renew. Sustain. Energy Rev.*, vol. 110, pp. 467–484, 2019.
- [57] A. Fallahi, G. Guldentops, M. Tao, S. Granados-Focil, and S. Van Dessel, “Review on solid-solid phase change materials for thermal energy storage: Molecular structure and thermal properties,” *Appl. Therm. Eng.*, vol. 127, pp. 1427–1441, 2017.
- [58] D. K. Benson, J. D. Webb, R. W. Burrows, J. McFadden, and C. Christensen, “Materials research for passive solar systems: solid-state phase-change materials,” Solar Energy Research Inst., Golden, CO (USA), 1985.
- [59] A. Bayon, M. Liu, D. Sergeev, M. Grigore, F. Bruno, and M. Müller, “Novel solid–solid phase-change cascade systems for high-temperature thermal energy storage,” *Sol. Energy*, vol. 177, pp. 274–283, 2019.
- [60] K. Nishioka, N. Suura, K. Ohno, T. Maeda, and M. Shimizu, “Development of Fe base phase change materials for high temperature using solid–solid transformation,” *ISIJ Int.*, vol. 50, no. 9, pp. 1240–1244, 2010.
- [61] G. Guldentops, G. Ardito, M. Tao, S. Granados-Focil, and S. Van Dessel, “A numerical study of adaptive building enclosure systems using solid–solid phase change materials with variable transparency,” *Energy Build.*, vol. 167, pp. 240–252, 2018.
- [62] Q. Y. Yan and L. L. Jin, “Research on the thermal storage performance of solid-solid phase-change material used in the wall,” in *Advanced Materials Research*, 2012, vol. 347, pp. 2801–2804.
- [63] P. Khomein *et al.*, “Random copolymer of poly (polyethylene glycol methyl ether) methacrylate as tunable transition temperature solid-solid phase change material for thermal energy storage,” *Sol. Energy Mater. Sol. Cells*, vol. 225, p. 111030, 2021.
- [64] P. C. Tabares-Velasco, C. Christensen, and M. Bianchi, “Verification and validation of EnergyPlus phase change material model for opaque wall assemblies,” *Build. Environ.*, vol. 54,

- no. July, pp. 186–196, 2012.
- [65] S. N. Al-Saadi and Z. Zhai, “Systematic evaluation of mathematical methods and numerical schemes for modeling PCM-enhanced building enclosure,” *Energy Build.*, vol. 92, pp. 374–388, Apr. 2015.
- [66] A. Castell, M. Medrano, and F. Goia, “Modelling Envelope Components Integrating Phase Change Materials (PCMs) with Whole-Building Energy Simulation Tools: a State of the Art,” *J. Facade Des. Eng.*, vol. 6, no. 3, pp. 132–148, 2018.
- [67] C. Curcija, S. Vidanovic, R. Hart, J. Jonsson, and R. Mitchell, “WINDOW Technical Documentation,” *Lawrence Berkeley Natl. Lab.*, 2018.
- [68] D. B. Crawley *et al.*, “EnergyPlus: Creating a new-generation building energy simulation program,” *Energy Build.*, vol. 33, no. 4, pp. 319–331, 2001.
- [69] E. Moreles, G. Huelsz, and G. Barrios, “Hysteresis effects on the thermal performance of building envelope PCM-walls,” in *Building Simulation*, 2018, vol. 11, no. 3, pp. 519–531.
- [70] Q. Zheng, S. Kaur, C. Dames, and R. S. Prasher, “Analysis and improvement of the hot disk transient plane source method for low thermal conductivity materials,” *Int. J. Heat Mass Transf.*, vol. 151, p. 119331, 2020.
- [71] K. Faraj, M. Khaled, J. Faraj, F. Hachem, and C. Castelain, “A review on phase change materials for thermal energy storage in buildings: Heating and hybrid applications,” *J. Energy Storage*, p. 101913, 2020.

Appendix A Equivalent window dimensions

The models in Figure 1c and d are designed to have equal thickness (l) and area (S).

$$l_{eWG} = l_{WG} + l_{tPCM} \quad (1)$$

$$l_{ePCM} = l_{tPCM} \quad (2)$$

$$l_{TIM} = l_{WG} \quad (3)$$

$$S_{WG} = S_{tPCM} \quad (4)$$

$$S_{TIM} = S_{ePCM} \quad (5)$$

$$S_{TIM} + S_{eWG} = S_{WG} \quad (6)$$

Here, the subscript “e” indicates “equivalent”. The thicknesses used in the equivalent model simulation are $l_{eWG} = 27.1$ mm, $l_{TIM} = 24.1$ mm, $l_{ePCM} = 3$ mm, as labeled in Figure 1. The thicknesses are held constant in this parametric study.

Appendix B Equivalent solar absorption and transmission

The models in Figure 1c and d are designed to have equal absorbed and transmitted solar energy. We assume the equivalent PCM absorbs all the solar energy that is transmitted from TIM in front of it. We have tested and confirmed that the position or lateral geometry design of the ePCM in Figure 1d (e.g., whether it occupies the top half or right half of the space) has no effect on the result and should be equivalent to the realistic case in Figure 1c due to the EnergyPlus algorithm. Symbols with prime are the optical parameters for components in the WG+tPCM system; hence α'_{tPCM} is different from α_{tPCM} , which indicates the solar absorptance of translucent PCM as a single layer. Based on the fundamental relationships between optical propagation properties in each case, we have,

$$r'_{WG+tPCM} + \alpha'_{WG} + \alpha'_{tPCM} + \tau'_{WG+tPCM} = 1 \quad (7)$$

$$r_{eWG} + \alpha_{eWG} + \tau_{eWG} = 1 \quad (8)$$

$$r_{TIM} + \alpha_{TIM} + \tau_{TIM} = 1 \quad (9)$$

$$\alpha_{ePCM} = 1 \quad (10)$$

By equating the transmitted, absorbed and reflected solar energy in the two cases, we have,

$$\tau_{eWG} S_{eWG} = \tau'_{WG+tPCM} S_{WG} \quad (11)$$

$$\tau_{TIM} \alpha_{ePCM} S_{ePCM} = \alpha'_{tPCM} S_{tPCM} \quad (12)$$

$$r_{eWG} S_{eWG} + r_{TIM} S_{TIM} = r'_{WG+tPCM} S_{WG} \quad (13)$$

$$\alpha_{eWG} S_{eWG} + \alpha_{TIM} S_{TIM} = \alpha'_{WG} S_{WG} \quad (14)$$

In EnergyPlus simulation, since the PCM can only be opaque, $\alpha_{ePCM} = 1$ (hence $\tau_{ePCM} = r_{ePCM} = 0$), we vary the area of the ePCM, i.e., S_{ePCM} (which is the same as S_{TIM}) in the equivalent

model. We define R_S as the ratio of the area of equivalent opaque PCM to that of window glazing, i.e.,

$$R_S = \frac{S_{ePCM}}{S_{WG}} \quad (15)$$

We let the TIM to have the same optical properties as the equivalent window, i.e., $\tau_{TIM} = \tau_{eWG}$, $r_{TIM} = r_{eWG}$ and $\alpha_{TIM} = \alpha_{eWG}$. Then Appendix Eq. (13) becomes

$$r_{eWG}(S_{eWG} + S_{ePCM}) = r_{eWG}S_{WG} = r'_{WG+tPCM}S_{WG} \quad (16)$$

where we used Appendix Eq. (6), and hence

$$r_{eWG} = r'_{WG+tPCM} \quad (17)$$

From Appendix Eq. (14), $\alpha'_{WG}S_{WG} = \alpha_{eWG}(S_{eWG} + S_{TIM}) = \alpha_{eWG}S_{WG}$, which gives

$$\alpha_{eWG} = \alpha'_{WG} \quad (18)$$

Then, from Appendix Eq. (4) and (12),

$$R_S = \frac{S_{ePCM}}{S_{WG}} = \frac{S_{ePCM}}{S_{tPCM}} = \frac{\alpha'_{tPCM}}{\tau_{TIM}\alpha_{ePCM}} = \frac{\alpha'_{tPCM}}{\tau_{eWG}} \quad (19)$$

therefore, by using Appendix Eq. (8), (17) and (18), we have

$$R_S = \frac{\alpha'_{tPCM}}{1-r_{eWG}-\alpha_{eWG}} = \frac{\alpha'_{tPCM}}{1-r'_{WG+tPCM}-\alpha'_{WG}} \quad (20)$$

where $r'_{WG+tPCM}$ and α'_{WG} are constants in this study. Therefore, R_S is proportional to α'_{tPCM} . The area S_{ePCM} (which always equals S_{TIM}) corresponding to R_S is varied in the equivalent model to account for the change of tPCM absorptance (α'_{tPCM} in the realistic model in Figure 1c) in our PCM parametric sweep based on Appendix Eq. (19).

Appendix C Equivalent thermal conductivity

The models in Figure 1c and 1d are designed to have equal thermal resistance. We use $k_{ePCM} = k_{tPCM}$ and $k_{TIM} = k_{WG}$, and this requirement gives

$$\frac{l_{eWG}}{k_{eWG}} = \frac{l_{WG}}{k_{WG}} + \frac{l_{tPCM}}{k_{tPCM}} \quad (21)$$

which then indicates

$$k_{eWG} = \frac{(l_{WG}+l_{tPCM})k_{WG}k_{tPCM}}{l_{WG}k_{tPCM}+l_{tPCM}k_{WG}} \quad (22)$$

Appendix D Equivalent thermal mass

The models in Figure 1c and 1d are designed to have equal thermal mass (C_{th}), which is defined as the product of the density and specific heat $C_{th} = mc_p = lS\rho c_p$. We set the thermal mass of

ePCM to be the same as tPCM. The value of c_p for each part is fixed at their original material property. Therefore,

$$l_{tPCM} S_{tPCM} \rho_{tPCM} c_p = l_{ePCM} S_{ePCM} \rho_{ePCM} c_p \quad (23)$$

Then the density of the equivalent opaque PCM is derived as

$$\rho_{ePCM} = \rho_{tPCM} \frac{S_{tPCM}}{S_{ePCM}} = \frac{\rho_{tPCM}}{R_S} \quad (24)$$